Check for updates

CsrA selectively modulates sRNA-mRNA regulator outcomes

Alejandra Matsuri Rojano-Nisimura[1†], Trevor R. Simmons[2†],
Abigail N. Leistra[2], Mia K. Mihailovic[2], Ryan Buchser[2],
Alyssa M. Ekdahl[2], Isabella Joseph[2], Nicholas C. Curtis[2] and
Lydia M. Contreras[1,2]*

[1]Biochemistry Graduate Program, University of Texas at Austin, Austin, TX, United States, [2]McKetta Department of Chemical Engineering, University of Texas at Austin, Austin, TX, United States

Post-transcriptional regulation, by small RNAs (sRNAs) as well as the global Carbon Storage Regulator A (CsrA) protein, play critical roles in bacterial metabolic control and stress responses. The CsrA protein affects selective sRNA-mRNA networks, in addition to regulating transcription factors and sigma factors, providing additional avenues of cross talk between other stress-response regulators. Here, we expand the known set of sRNA-CsrA interactions and study their regulatory effects. *In vitro* binding assays confirm novel CsrA interactions with ten sRNAs, many of which are previously recognized as key regulatory nodes. Of those 10 sRNA, we identify that McaS, FnrS, SgrS, MicL, and Spot42 interact directly with CsrA *in vivo*. We find that the presence of CsrA impacts the downstream regulation of mRNA targets of the respective sRNA. *In vivo* evidence supports enhanced CsrA McaS-*csgD* mRNA repression and showcases CsrA-dependent repression of the *fucP* mRNA via the Spot42 sRNA. We additionally identify SgrS and FnrS as potential new sRNA sponges of CsrA. Overall, our results further support the expanding impact of the Csr system on cellular physiology via CsrA impact on the regulatory roles of these sRNAs.

KEYWORDS

CsrA/RsmA, sRNA (small RNA), sRNA regulatory network, Posttranscriptional regulation, RNA-protein interactions

Introduction

Non-coding RNAs have emerged as potent regulators of gene expression in cellular metabolism and stress responses (Gottesman et al., 2006; Vazquez-Anderson and Contreras, 2013; Wagner and Romby, 2015; Leistra et al., 2019). In bacteria, one type of regulatory non-coding RNAs, small RNAs (sRNAs), bind and affect the expression of their target genes at the protein and RNA level. For example, antisense sRNAs regulate a target mRNA via an extended region of perfectly complementary nucleotides to alter translation or stability of the mRNA (Hör et al., 2020). Alternatively, trans-acting sRNAs, oftentimes encoded in intergenic regions in the DNA, recognize one or more target mRNAs via regions of 15–40 nucleotides of limited complementarity (Gottesman and Storz, 2011; Villa et al., 2017). These interactions result in a diversity of regulatory outcomes and mechanisms (reviewed in De Lay et al., 2013; Hör et al., 2020; Nitzan et al., 2017; Wagner and Romby, 2015).

Due to the vast regulatory functions of sRNAs, many efforts have been made to elucidate native regulatory roles of individual sRNAs (Vanderpool and Gottesman, 2004; Durand and Storz, 2010; Beisel and Storz, 2011; Thomason et al., 2012; Guo et al., 2014; Lalaouna et al.,
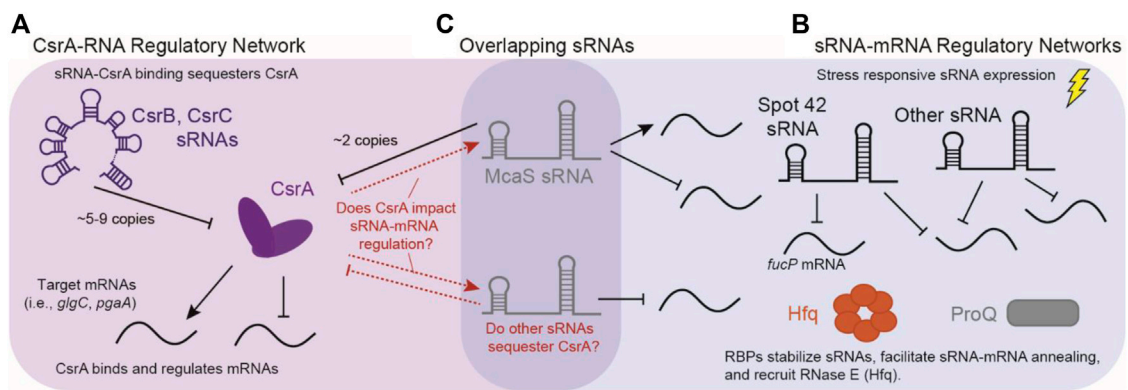
FIGURE 1
Overlap of sRNA-mRNA and CsrA-RNA post-transcriptional regulatory networks. **(A)** The canonical CsrA regulatory network: CsrA binds mRNA targets to either repress or activate translation. CsrA is then regulated by sRNAs CsrB and CsrB, which can sequester up to 9 and 5 copies of CsrA, respectively. **(B)** Concurrently, sRNAs regulate mRNAs targets in response to external stimuli, these interactions are assisted by RNA Binding Proteins (RBPs) such as Hfq and ProQ. **(C)** sRNAs such as McaS are overlapping sRNAs that both regulate mRNA targets, as well as CsrA. There is potentially many other sRNAs that can fall into both regulatory modes.

2015). In *Escherichia coli*, almost 100 sRNAs have been confirmed, targeting nearly 70 unique mRNAs, with 13 of these mRNAs regulated by multiple sRNAs (Hör et al., 2018; Mihailovic et al., 2018; J. Wang et al., 2016). In this paper, we define a confirmed mRNA target as one in which a regulatory outcome and binding interface has been determined experimentally (*i.e.*, reporter assays with compensatory mutations or *in vitro* binding assays). However, outside of this confirmed mRNA target pool, a much broader set of putative sRNA-mRNA interactions have been inferred from recent high-throughput studies (Melamed et al., 2016; 2020; Liu et al., 2017; Waters et al., 2017; Iosub et al., 2020). A complex, dynamic network of stress response and metabolic control emerges from these data (Figure 1A) (Wagner and Romby, 2015; Nitzan et al., 2017), that is believed, in many cases, to hinge on the Hfq chaperone protein (Vogel and Luisi, 2011; Kavita et al., 2018).

The hexameric Hfq protein is a global RNA-Binding Protein (RBP) that binds trans-acting sRNAs and their target mRNAs at well-characterized sequence motifs to facilitate inter-molecular base pairing (Holmqvist and Vogel, 2018). Several explanations have been proposed for the RNA chaperone function of Hfq, including but not limited to: 1) stabilization of the sRNA (Cameron et al., 2019), 2) facilitation of inter-molecular base pairing by unfolding RNA secondary structures, and 3) increase of the local sRNA concentration to augment mRNA pairing and regulation probability (Vogel and Luisi, 2011; Desnoyers and Massé, 2012; Wagner and Romby, 2013; Santiago-Frangos and Woodson, 2018). However, the specific role of Hfq in each sRNA-mRNA interaction seems to remain variable, with many sRNAs sufficient to disrupt mRNA translation without Hfq, predominantly when the sRNA directly occludes the ribosome binding site of the respective mRNA (Morita et al., 2006; Maki et al., 2008; Prevost et al., 2011). For Hfq-dependent sRNAs, it has been shown that some sRNAs compete with each other for binding sites under Hfq-limited cellular conditions (Santiago-Frangos et al., 2016), suggesting complex and dynamic global post-transcriptional networks.

Despite the extensive regulatory role of Hfq across bacterial post-transcriptional networks, this protein is not the only global

RBP that influences sRNA-mediated post-transcriptional regulation. More recently, the FinO-like protein ProQ was discovered as a global RBP through Grad-Seq (Figure 1A). Like Hfq, ProQ has been shown to facilitate sRNA-mRNA interactions directly (Smirnov et al., 2016; Smirnov et al., 2017; Holmqvist et al., 2018), although using structural-specificity as opposed to sequence-specificity. RIL-Seq results show that in *E. coli*, ProQ and Hfq have approximately 100 shared target sRNA-mRNA pairs (Melamed et al., 2020). However, some organisms with documented trans-acting sRNAs-mRNA target pairs lack both Hfq and ProQ altogether; some examples include Gram positive bacteria *Deinococcus radiodurans* (Tsai et al., 2015; Villa et al., 2021) and *Mycobacterium tuberculosis* (Dichiara et al., 2010; Gerrick et al., 2018; Taneja and Dutta, 2019). In such organisms, KH domain proteins have started to gain attention as potential matchmaking RBPs (Olejniczak et al., 2022) due to their ability to associate with sRNAs (Hör et al., 2020; Lamm-Schmidt et al., 2021). This reinforces the notion that other RBPs may be involved in sRNA-mRNA regulation (Haning et al., 2014; Smirnov et al., 2016; Hör et al., 2020).

Another identified RBP candidate for sRNA-mRNA regulation is the Carbon Storage Regulatory A protein (CsrA). CsrA is the major protein regulator of the Carbon Storage Regulatory (Csr) Network, also known as the Rsm (Regulator of Secondary Metabolites) Network. Overall, the Csr network represses stationary phase processes, including biofilm formation and glycogen synthesis, while activating exponential phase processes such glycolysis and motility (Romeo and Babitzke, 2018). CsrA is a global RBP widely conserved in the *Gammaproteobacteria* class as well as in the *Firmicutes* and *Planctomycetes* phyla (Finn et al., 2014; Valkulskas et al., 2015). CsrA predominantly acts by repressing translation of mRNAs (Figure 1B) by directly occluding the ribosome binding site via binding of a conserved "A(N)GGA" motif contained within a hairpin structure; however, additional cases of CsrA binding and activation of mRNA targets are also documented (Ren et al., 2014; Renda et al., 2020). Molecularly,

the GGA triplet sequence has been identified as the most critical feature for CsrA binding (Dubey et al., 2005); from here we will refer to this as the "GGA Motif". In *E. coli*, expression of two sRNAs, CsrB and CsrC, antagonize CsrA regulation through binding and sequestration, resulting in the titration of intracellular CsrA concentrations (Romeo et al., 2013; Leng et al., 2016). The CsrB and CsrC sponge sRNAs have multiple copies of the hairpin contained GGA motif and bind CsrA in stoichiometric ratios up to 9:1 and 5:1, respectively (M. Y. Liu and Romeo, 1997; Weilbacher et al., 2003). One additional sRNA known to sequester CsrA is McaS, albeit to a lesser extent than CsrB and CsrC (Figure 1C) (Kavita et al., 2018). McaS contains four copies of the GGA CsrA binding motif and can bind two copies of CsrA *in vitro*. Additionally, it co-purifies with CsrA *in vivo* (Jorgensen et al., 2013). So far, this sequestration and titration of CsrA has been the main function attributed to CsrA-sRNA interactions in the literature.

In recent years, high-throughput characterizations of the Csr system in *Salmonella* and *E. coli,* identified several additional sRNAs that could directly interact with the CsrA protein (Figure 1C) (Holmqvist et al., 2016; Potts et al., 2017; Sowa et al., 2017). Additionally, during the preparation of this manuscript the sRNA Spot42 was identified to have CsrA-dependent interactions, in which CsrA occludes an RNAse E degradation site to prevent degradation (Lai et al., 2022). The implication of CsrA-Spot42 interactions is particularly interesting due to the many roles of Spot42 sRNA in cell regulation (Sahagan and Dahlberg, 1979; Beisel and Storz, 2011; Aoyama et al., 2022). Lastly, work in *Bacillus subtilis* also supports that CsrA-sRNA interactions may play a direct role in impacting sRNA-mRNA regulation (Müller et al., 2019). Given documented sRNA association (Valkulskas et al., 2015) and 2) broad conservation (Romeo and Babitzke, 2018), it has been proposed that CsrA could fulfill a broader regulatory role within sRNA-regulated networks, particularly in organisms lacking Hfq and ProQ, such as *Bacillus subtills* (Müller et al., 2019).

In this work, we investigate potential direct interactions and regulatory dependence of sixteen sRNAs with CsrA in *E. coli*; these sRNAs were originally identified by computational prediction studies (SI Table 3) and CLIP studies (Potts et al., 2017; Sowa et al., 2017). Of the initial 16 sRNAs, we demonstrate 10 novel sRNA-CsrA binding interactions *in vitro,* interestingly some of which do not contain the canonical GGA motif. From this subset, we systematically evaluate the ability of these sRNAs to affect CsrA-mRNA regulation *in vivo* by utilizing overexpression fluorescent reports assays. We also investigate the ability of CsrA to impact the regulatory roles of the sRNAs on their respective target mRNAs. Two sRNAs (FnrS and SgrS) were discovered to serve as sponges and sequester CsrA with reduced levels of "sponging activity" relative to that of the CsrB and CsrC sRNAs when expressed from inducible promoters and from *in vivo* reporter-based assays. Additionally, we found that the presence of CsrA uniquely impacts regulatory activity of three sRNAs (McaS, MicL and Spot42) on their respective mRNA targets. For instance, CsrA enhances McaS-*csgD* and is required for Spot42-*fucP* repression. As a whole, our work expands the post-transcriptional regulatory roles of CsrA beyond its traditional (mRNA-focused) modes of regulation.

Results

Identifying additional sRNAs implicated in CsrA regulatory interactions

We compiled a list of 16 sRNAs (Table 1), outside of CsrB, CsrC, and McaS. The set of potential CsrA-binding sRNAs in Table 1 encompasses the diverse activity of known sRNAs in *E. coli*. These sRNAs were compiled and reanalyzed from previous data showing sRNA-CsrA interactions; these include CsrA CLIP-Seq (Potts el al., 2017), HITS-CLIP (Sowa et al., 2017) and differentially expression data in *E. coli* (Sowa et al., 2017) (described in Materials and Methods). Eleven of the 16 sRNAs are trans-acting sRNAs that have at least one confirmed mRNA target (Table 1; Supplementary Table S1) and many are associated with specific stress responses or metabolic pathways (Supplementary Table S2). As a note, three of these sRNAs do not contain a GGA binding motif and may be interacting through degenerate GGN-like sequences. To identify putative binding sites, we applied a previously developed biophysical model of CsrA-RNA interaction (Leistra et al., 2018). A full computational workflow for using the model is in the Materials and Methods. While some of these sRNAs have been tested for CsrA binding *in vitro* (summarized in Table 1), potential *in vivo* regulatory interactions with CsrA have not been considered, excluding McaS, CsrB, and CsrC. McaS and CsrB are included as positive controls because of their previously established sponge activity for CsrA (Dubey et al., 2005; Jorgensen et al., 2013). McaS is considered especially relevant as it contains 4 copies of the GGA motif which is on the same order of magnitude as the other sRNAs of interest; this is in contrast to CsrB, which contains 22 copies of the hairpin-contained GGA motif and is therefore assumed to bind CsrA with higher affinity.

However, it is important to note, that the sequence and structural features of the motif are not strict requirements for CsrA binding as degenerate GGA-like sequences may contribute to CsrA-RNA binding and regulation in some target mRNAs. For instance, CsrA binds at non-stem loop GGA sequences in *cstA in vitro* (Dubey et al., 2003) and degenerate GGA-like sequences are thought to contribute to CsrA-RNA binding and regulation of some targets (Kulkarni et al., 2014; Leistra et al., 2018; Mercante et al., 2009; X. Wang et al., 2005; H. Yakhnin et al., 2011).

Ten novel sRNA binding partners are confirmed for CsrA *in vitro*

We first assessed whether the 16 identified sRNAs bound CsrA *in vitro* using electrophoretic mobility shift assays (EMSA). CsrA was purified as described in the Materials and Methods and purity was assessed by SDS-PAGE (Supplementary Figure S1). For these experiments, 10 nM of P^{32} - radiolabeled sRNAs were incubated with 3 μM or 6 μM of CsrA, which produced a CsrA: sRNA molar ratio of 300:1 and 600:1, respectively. These ratios were selected based on the reported binding affinities for Spot42, GadY, GcvB, and MicL presumed to be physiologically relevant via CsrA CLIP-Seq data (Potts et al., 2017). Additionally, all binding assays are performed in large excess of yeast total

TABLE 1 A summary of sRNAs implicated in the Csr system.

sRNA	Differential Expression ΔcsrBC strain Sowa et al. (2017)	Prior *in vivo* CsrA binding evidence (CLIP-seq/o HITS-CLIP) Potts et al. (2017), Sowa et al. (2017)	Prior *in vitro* CsrA binding evidence (EMSA)	Total GGAs (# in loop of a SL)	Type
SgrS	yes	yes		2 (0)	trans-acting
RnpB	yes	yes		7 (1)	catalytic
GlmZ	yes	yes		2 (0)	trans-acting
SibD	yes	yes		3 (1)	antisense
GadY	yes	yes	yes Potts et al. (2017)	2 (1)	antisense
SibA	yes	yes		3 (2)	antisense
GcvB	yes	yes	yes Potts et al. (2017), no Jorgensen et al. (2013)	2 (0)	trans-acting
SibC	yes	yes		2 (1)	antisense
ChiX	not detected	yes	no, yes with Hfq2	0 (0)	trans-acting
McaS	not detected		yes, yes with Hfq Jorgensen et al. (2013), Darnell (2010)	4 (2)	trans-acting
RprA	not detected		weak, yes with Hfq2	1 (0)	trans-acting
MicL (MicL-S)	N/A	yes	yes Potts et al. (2017) (MicL-long)	0 (0)	trans-acting
FnrS	N/A	yes	no Potts et al. (2017)	0 (0)	trans-acting
Spot 42 (spf gene)	no	yes	yes Potts et al. (2017)	1 (0)	trans-acting
CyaR	no	yes	no Potts et al. (2017)	1 (1)	trans-acting
DsrA	no	yes	weak, yes with Hfq2	1 (0)	trans-acting
CsrB[3]	yes	yes	yes Liu et al. (1997); Weilbacher et al. (2003)	22 (14)	protein sponge
CsrB[3]	yes	yes	yes Weilbacher et al. (2003)	14 (4)	protein sponge

Footnotes: [1]Number in parenthesis indicates number of GGA, sequences present in loop sequences of predicted stem loop (SL) RNA, structures, [2]Personal communication Dr. sarah woodson, [3]CsrB and CsrC are included for reference.

RNA, which has been previously shown to inhibit non-specific association of CsrA to labeled sRNA (A. V Yakhnin et al., 2012).

Across all conditions, super-shifted complexes indicating CsrA binding were detected upon addition of CsrA for 14 of 16 sRNAs (Figure 2; Supplementary Figure S2). Clear *in vitro* CsrA binding not yet been reported in the literature was detected for several sRNAs: SgrS, ChiX, RprA, DsrA, and SibA (Figures 2A, B, D, E; Supplementary Figure S2D). In addition to these five novel interactions, the sRNAs Spot 42, GadY, and McaS bound CsrA (Figures 2G–I) as has been previously shown, which gives confidence to our EMSA conditions generating true novel sRNA-CsrA interactions. We also observed CsrA binding to MicL, RnpB, GlmZ and SibD at the 6 μM concentration of CsrA, which we believe to be sufficient evidence of *in vitro* CsrA interaction (Supplementary Figures S2A, B, C, E1). It is worth

noting that stronger *in vitro* CsrA binding has been previously detected for MicL (Potts et al., 2017); however, this prior study utilized the full-length sequence (MicL-long), while we tested the short, 5′-processed MicL-S sequence (referred to here as MicL for simplicity). The latter is thought to be the functionally active form of the sRNA (Guo et al., 2014). In contrast, CsrA binding was not detected for the GcvB and SibC sRNAs (Supplementary Figures S2F, G). Full EMSA images are included in Supplementary Figure S3.

Recently, co-immunoprecipitation study of Hfq in *E. coli* demonstrated that CsrA co-precipitates with Hfq in an RNA-dependent manner (Caillet et al., 2019). To qualitatively assess if sRNAs from this set can bind both CsrA and Hfq *in vitro* and/or if Hfq influenced CsrA-sRNA binding, we tested binding of all the 16 sRNAs with CsrA (6 μM) in the presence of different Hfq
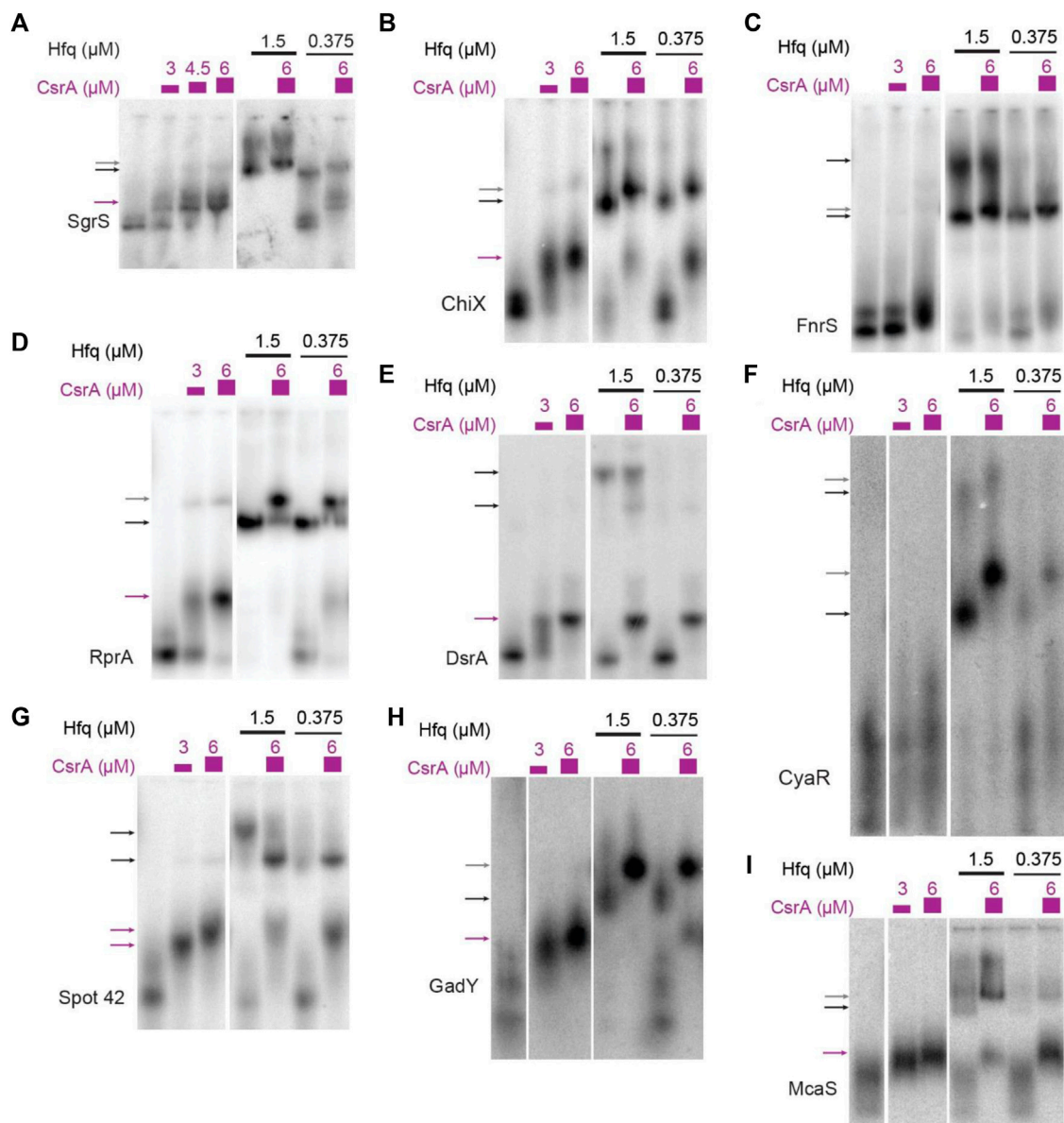
FIGURE 2
sRNAs bind CsrA *in vitro*. *In vitro* evaluation of 14 sRNAs with CsrA using Electrophoretic Mobility Shift Assays (EMSAs). These assays were performed by titrating CsrA concentrations (purple), as well as in the presence and absence of Hfq (black). The sRNAs tested are as follows: **(A)** SgrS, **(B)** ChiX, **(C)** FnrS, **(D)** RprA, **(E)** DsrA, **(F)** CyaR, **(G)** Spot42, **(H)** GadY, **(I)** McaS. Arrows indicate bound complexes: CsrA-RNA complexes (purple), Hfq-RNA complexes (black), ternary CsrA-Hfq-RNA complexes (gray).

concentrations (0.375 μM or 1.5 μM). These concentrations were selected to mimic estimated ratios natively occurring between these two proteins *in vivo* (Materials and Methods). Importantly, we found that the presence of Hfq affected the binding of many sRNAs to CsrA, likely forming ternary complexes of CsrA-sRNA-Hfq (Figures 2A–E, H, I). These results agree with prior *in vitro* observation of ternary CsrA-sRNA-Hfq complexes for ChiX, RprA, and McaS (Jorgensen et al., 2013; Peng, 2014 and Dr. S Woodson, personal communication, August 2018). The complete summary of the EMSA results is compiled in Table 2. In total, we demonstrate 10 novel, and 14 total sRNA-CsrA interactions *in vitro*.

In vivo sRNA screen identifies CsrA-sequestration activity for FnrS and SgrS

We next investigated the *in vivo* functional implications of the *in vitro* confirmed CsrA-sRNA interactions. We consider two non-exclusive hypotheses: 1) the possibility that sRNAs are minor antagonists of CsrA similar to CsrB and CsrC and 2) the possibility that sRNA-CsrA binding regulates downstream sRNA-mRNA target interactions. As such, we initially pursued 12 of the 14 sRNAs that 1) bound CsrA *in vitro* and 2) had some evidence of CsrA impact *in vivo* (Summarized in Table 2). We excluded SibA and SibD as these sRNAs proved difficult to work with *in vivo* due to

TABLE 2 Summarized *in vitro* sRNA-CsrA binding results from EMSAs.

sRNA	Bind CsrA *in vitro*	Summary of *in vivo* evidence	Novel *in vitro* interaction?	Selected for *in vivo* assays?
McaS	Yes	Jorgensen et al. (2013), HITS-CLIP		Yes
GadY	Yes	CLIP-SeqDE, HITS-CLIP		Yes
Spot 42 (*spf* gene)	Yes	TriFC, CLIP-Seq, HITS-CLIP		Yes
SibA	Yes	DE, HITS-CLIP	*	Yes‡
ChiX	Yes	TriFC	*	Yes
SgrS	Yes	DE, HITS-CLIP	*	Yes
MicL (MicL-S)	Yes	CLIP-Seq		Yes
RprA	Yes	NONE	*	
DsrA	Yes	HITS-CLIP	*	
RnpB	Yes†	DE, HITS-CLIP	*	Yes
GlmZ	Yes†	DE, HITS-CLIP	*	Yes
SibD	Yes†	DE, HITS-CLIP	*	Yes‡
FnrS	Yes (only detected clearly + Hfq)	CLIP-Seq	*	Yes
CyaR	Yes (only detected clearly + Hfq)	CLIP-Seq, HITS-CLIP	*	Yes
GcvB	NO	DE, CLIP-Seq, HITS-CLIP		
SibC	NO	DE, HITS-CLIP		

Footnotes: "Jorgenson et al., 2013" provides molecular insights on the McaS-CsrA interaction. "CLIP-seq" refers to positive hits in Potts et al., 2017. "DE" refers to differential expression in Sowa et al., 2017, "HITS-CLIP" refers to positive hits in Sowa et al., 2017.
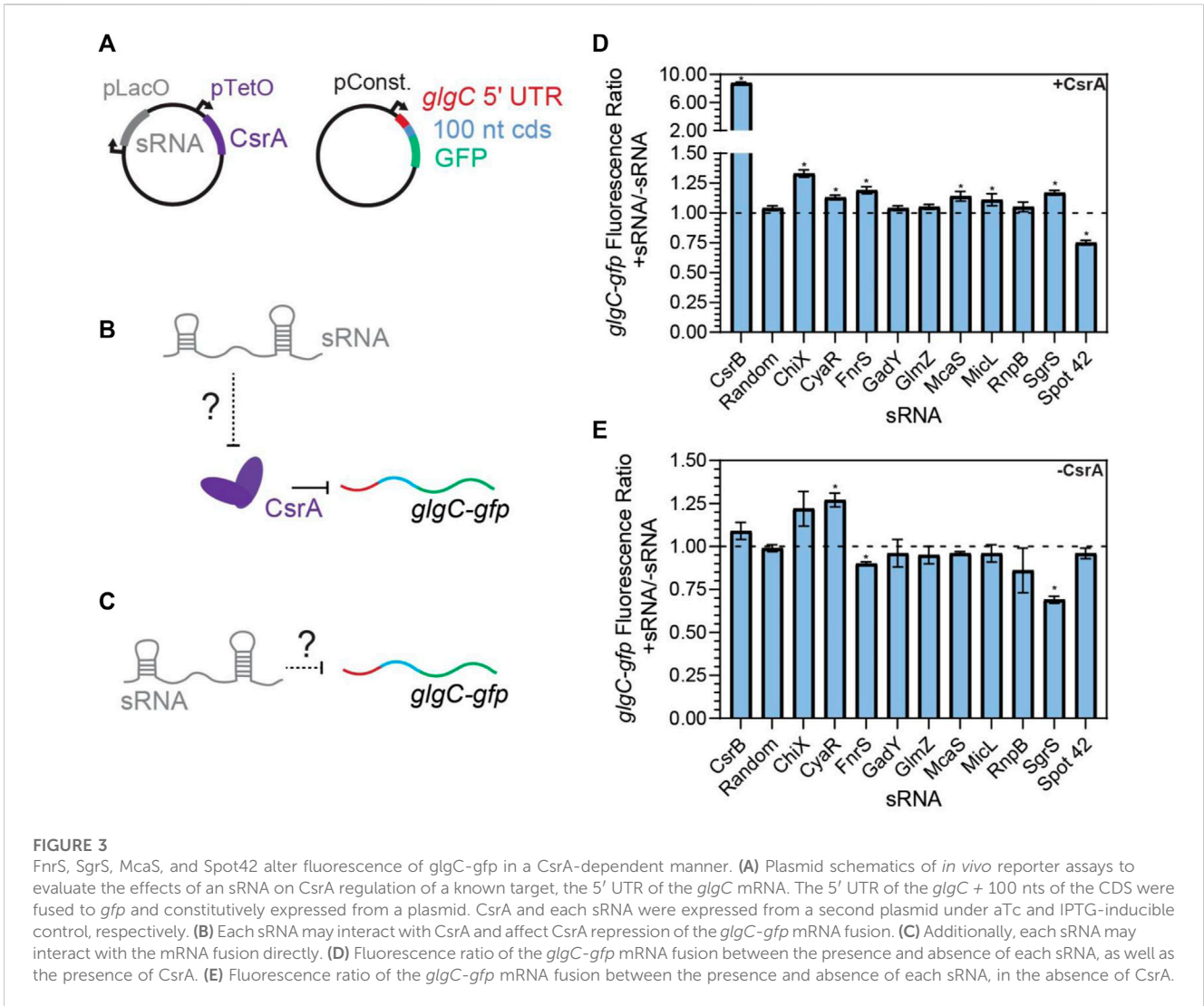
toxic peptide function [(Fozo et al., 2008; Brantl and Jahn, 2015) see Materials and Methods]. This ultimately left us with 10 total sRNAs to pursue in these assays: McaS, GadY, Spot42, ChiX, SgrS, MicL, RnpB, GlmZ, FnrS, and CyaR.

To evaluate if the found *in vitro* binding interactions could be directly recapitulated *in vivo*, we employed a plasmid-based fluorescence complementation system previously developed in our lab and previously shown to capture CsrA-CsrB interactions (Gelderman et al., 2015; Sowa et al., 2017; Mihailovic et al., 2021). Under the conditions tested, we were only able to detect a significant increase in GFP complementation (indicative of sRNA-CsrA proximity) for Spot42-CsrA and ChiX-CsrA, relative to the case of CsrA and a random sRNA sequence control (Supplementary Figure S4B). While allowing us to validate the new *in vivo* interaction between ChiX and CsrA, the YFP complementation signal was low even for the McaS positive control. This may be due to the large MS2 binding protein affecting RNA folding. Thus, these results suggest the need for a more sensitive *in vivo* approach to investigate the *in vitro* supported sRNA-CsrA interactions.

As observed previously for CsrB, CsrC, and McaS (Jorgensen et al., 2013; M. Y. Liu et al., 1997; Weilbacher et al., 2003), we anticipated that some of the novel sRNA-CsrA interactions would fall into our first hypothesis and act as a sponge sRNA and sequester CsrA *in vivo*. The sponging would then impact regulation of CsrA on its mRNA targets. To screen for this sponge activity of each sRNA, we adapted a plasmid-based screen previously utilized in our lab (Sowa et al., 2017; Leistra et al., 2018). In short, we induced expression of each sRNA with a constitutively expressed *glgC-gfp* translational fusion reporter both K-12 MG1655 wild type *E. coli* and a Δ*csrBCD csrA::kan* strain (*i.e.*, Csr system deletion strain). The *glgC-gfp* fusion was selected as CsrA binds

and represses translation of the *glgC* mRNA and *glgC* is one of the most well-characterized mRNA targets of CsrA (Baker et al., 2002; Mercante et al., 2009; Sowa et al., 2017). As a negative control, a random 80 nt sequence absent of any GGA motifs was selected from the *E. coli* genome (Supplementary Tables S1–S4). In this system, if a specific sRNA sequesters CsrA (diluting its effective concentration), we expect to observe an increase in fluorescence (indicative of less repressed *glgC-gfp* expression) following sRNA induction, relative to the fluorescent output of the uninduced system.

Screening revealed that CsrB, McaS, SgrS, and FnrS all significantly increased fluorescence of the *glgC-gfp* translational fusion only in the presence of induced CsrA (Figures 3D, E, *p*-value <0.05). While CsrB and McaS are positive controls and were expected, SgrS and FnrS are novel findings. Induction of CyaR and ChiX increased *glgC-gfp* fluorescence in the presence of CsrA (Figure 3D, *p*-value <0.05 by paired *t*-test), they also do so in the absence of CsrA (Figure 3E, *p*-value <0.05 and *p*-value =0.06), suggesting that these sRNAs may regulate the translational reporter directly or indirectly via a non-CsrA factor. In fact, CyaR has been reported to directly base-pair with the *glgC* transcript in RIL-seq experiments (Melamed et al., 2020). While ChiX has not been shown to directly target *glgC*, IntaRNA (Busch et al., 2008) predicts a base-pairing region between the two RNAs with a predicted ΔG of −5.83 kcal/mol; this is on the same scale as the IntaRNA prediction for the known IntaRNA ChiX-*chiP* interaction (ΔG of −4.82 kcal/mol), suggesting a potential direct interaction between ChiP and the *glgC* transcript (Mann et al., 2017). Surprisingly, GadY does not exhibit sponge activity for CsrA in our assays, as previously reported (Parker et al., 2017). This discrepancy may be explained by the lower copy number, and

FIGURE 3
FnrS, SgrS, McaS, and Spot42 alter fluorescence of glgC-gfp in a CsrA-dependent manner. **(A)** Plasmid schematics of *in vivo* reporter assays to evaluate the effects of an sRNA on CsrA regulation of a known target, the 5′ UTR of the *glgC* mRNA. The 5′ UTR of the *glgC* + 100 nts of the CDS were fused to *gfp* and constitutively expressed from a plasmid. CsrA and each sRNA were expressed from a second plasmid under aTc and IPTG-inducible control, respectively. **(B)** Each sRNA may interact with CsrA and affect CsrA repression of the *glgC-gfp* mRNA fusion. **(C)** Additionally, each sRNA may interact with the mRNA fusion directly. **(D)** Fluorescence ratio of the *glgC-gfp* mRNA fusion between the presence and absence of each sRNA, as well as the presence of CsrA. **(E)** Fluorescence ratio of the *glgC-gfp* mRNA fusion between the presence and absence of each sRNA, in the absence of CsrA.
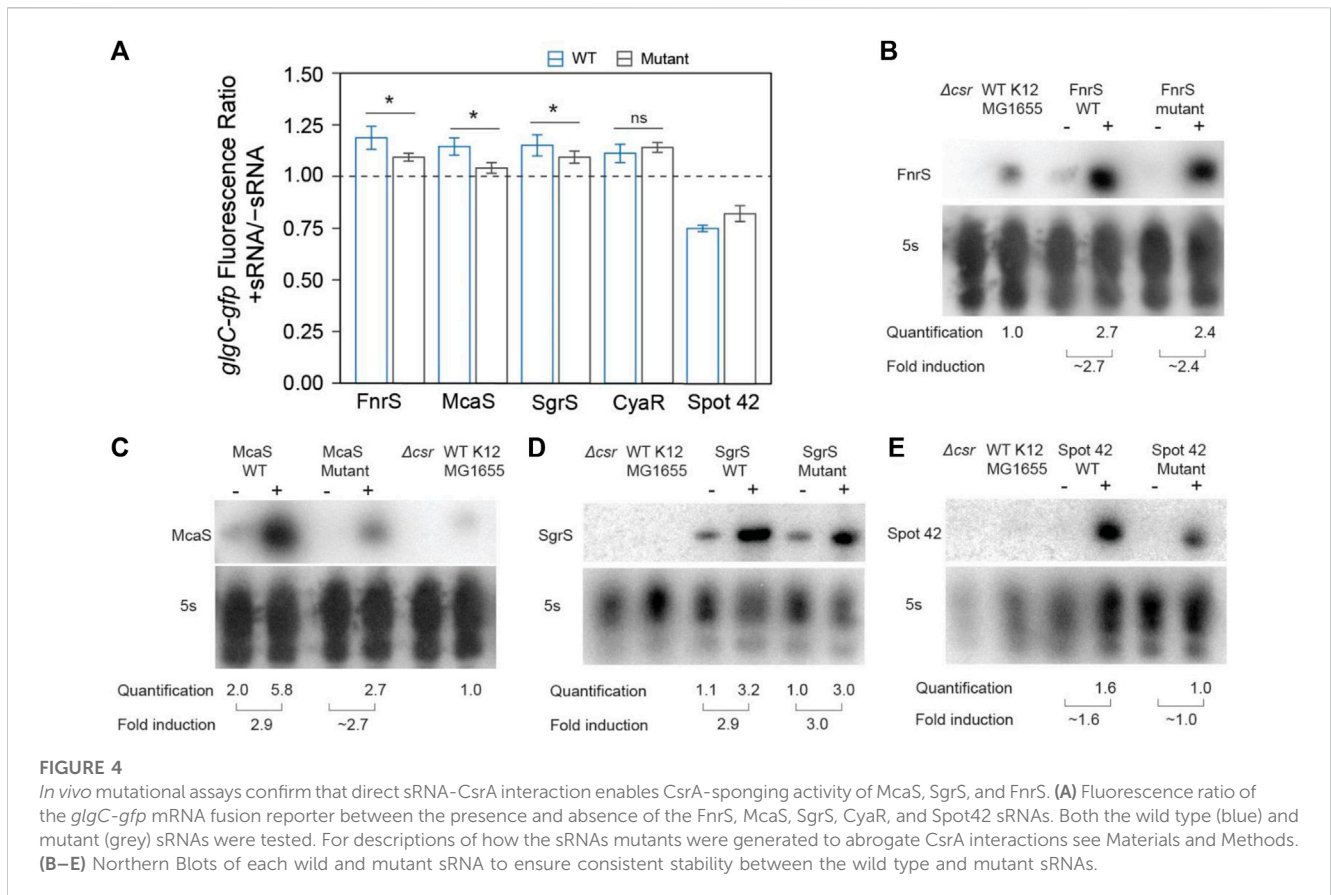
thus greater sensitivity, of the CsrA target reporter in the previous work.

To further evaluate the hypothesis that SgrS and FnrS are two novel CsrA sponge sRNAs, we interrupted putative CsrA binding sites within these sRNAs expecting this would abrogate CsrA sponge activity. McaS was used as a positive control in these experiments, given its earlier 1) demonstration of CsrA sponge activity, 2) confirmation of CsrA binding sites, and 3) more similar number of GGA motifs (compared to CsrB). Likewise, CyaR was used as a negative control because we anticipated that disrupting putative CsrA binding sites would not impact the likely CsrA-independent observed increase in *glgC-gfp* fluorescence (Figures 3D, E). For the sRNAs that contain one or more instances of the conserved GGA binding motif, we performed GGA:CCA mutations as done in previous literature to interrupt CsrA-RNA binding (Dubey et al., 2005; Patterson-Fortin et al., 2013). It should be noted that alternative mutations were made to the GGA motif if the standard GGA:CCA mutation altered the predicted secondary structure of the sRNA (Materials and Methods). We disrupted each instance of the GGA motif in the SgrS and CyaR sRNAs (termed "GGA mutants", Supplementary Table S4). For McaS, the

two GGA motifs (of 4 total) that were shown to be CsrA binding sites *in vitro* and *in vivo* in a previous study (Jorgensen et al., 2013) were mutated ("dual GGA mutant," Supplementary Tables S1–S4). For FnrS, which does not contain a GGA motif, GGN sequences within the most likely pair of putative CsrA binding sites predicted using the biophysical model (Supplementary Table S3) were mutated ("GGN mutant 1," Supplementary Table S4).

The mutant sRNAs were screened in the same plasmid assay. Induction of mutant FnrS, SgrS, and McaS mutant sRNAs significantly reduced fold increase of *glgC-gfp* fluorescence relative to the corresponding wild type sRNA (Figure 4A). Northern blotting analysis of these samples indicated both the wild type and mutant sRNAs are induced at comparable levels (Figures 4B–D). These data agree with a previous study of McaS, where mutations of the same GGA motifs significantly decreased its CsrA sponge activity, as measured by a *pgaA-lacZ* reporter (Jorgensen et al., 2013). Additionally, as expected, the CyaR mutant sRNA does not alter *glgC-gfp* fluorescence between the wild type and mutant sRNAs (Figure 4A), supporting the hypothesis that the observed effects of CyaR on *glgC-gfp* fluorescence (Figures 3D, E) do not involve direct CyaR-CsrA

FIGURE 4

In vivo mutational assays confirm that direct sRNA–CsrA interaction enables CsrA-sponging activity of McaS, SgrS, and FnrS. **(A)** Fluorescence ratio of the *glgC-gfp* mRNA fusion reporter between the presence and absence of the FnrS, McaS, SgrS, CyaR, and Spot42 sRNAs. Both the wild type (blue) and mutant (grey) sRNAs were tested. For descriptions of how the sRNAs mutants were generated to abrogate CsrA interactions see Materials and Methods. **(B–E)** Northern Blots of each wild and mutant sRNA to ensure consistent stability between the wild type and mutant sRNAs.

interactions. Lastly, altering the known GGA motif in Spot42 and expressing the mutant sRNA slightly alleviates the fold-repression effect observed when using the wild type Spot42 sRNA sequence, though that difference is not statistically significant (Figure 4A). This does point to the idea that the decrease in *glgC-gfp* fluorescence upon expression of Spot42 relies upon a direct CsrA-sRNA interaction.

The above data indicate that SgrS and FnrS can exert CsrA sponge activity similar to that of McaS in a plasmid-based system. However, the effects of these sRNAs on *glgC-gfp* fluorescence are relatively small (~1.2-fold increases) (Figure 4A) compared to that observed for CsrB (~9-fold increase) (Figure 3D). This drastic difference is expected, as CsrB contains 22 GGA CsrA binding motifs while McaS, Sgrs, and FnrS contain only 4 CsrA binding motifs at most (Summarized in Table 1). It is important to recognize that these results were collected using a plasmid-based expression system. To evaluate physiological sponge activity of SgrS, we took two approaches. First, we tracked *flhD-gfp* expression in the presence and absence of genomically-expressed SgrS as induced the presence of *a*-methyl glucoside (Walder and Vanderpool, 2007); *flhD* is a well characterized (stabilized) mRNA target of CsrA (Yakhnin et al., 2011). Therefore, the reduction in fluorescence when tracking expression of the *flhD-gfp* reporter in the presence of SgrS (relative to the same condition without SgrS), that we observed in Supplementary Figure S13B, indicated increased in SgrS-dependent CsrA sequestration (Figure 5; Figure 6; Supplementary Figure S7). To ensure these results depended on direct CsrA-SgrS interaction, we also conducted these experiments using a SgrS

mutant which had its predicted CsrA binding site mutated and observed no change in *flhD-gfp* reporter signal (Supplementary Figure S13C). Collectively, these data supported the notion that SgrS acts as sponge sRNA of CsrA under physiologically relevant conditions. It is worth noting that the *flhD-gfp* fusion was expressed from a promoter previously used for mimicking physiological mRNA expression levels (Adamson and Lim, 2013). The presence and absence of SgrS was induced using growth conditions previously confirmed to alter native levels of this sRNA (Wadler and Vanderpool, 2007); we confirmed that SgrS expression was significantly upregulated under these conditions using RT-qPCR analysis (Supplementary Figure S13D). We could not confirm native FnrS sponge activity as native increase in FnrS expression requires anaerobic growth conditions, which we were not able to confirm by RT-qPCR in consistency with previous works (Durand and Storz, 2010). Conditions in which FnrS is expressed natively is an ongoing area of interest for the field and will be useful for evaluating the ability for FnrS to act as a sponge for CsrA; identification of physiological conditions where FnrS sequesters and titrates CsrA away from its targets remains an outstanding question from this work.

CsrA impacts regulatory activity of the McaS sRNA on its mRNA targets

We next evaluated our second hypothesis: that CsrA remodels the downstream regulatory interactions of the sRNA
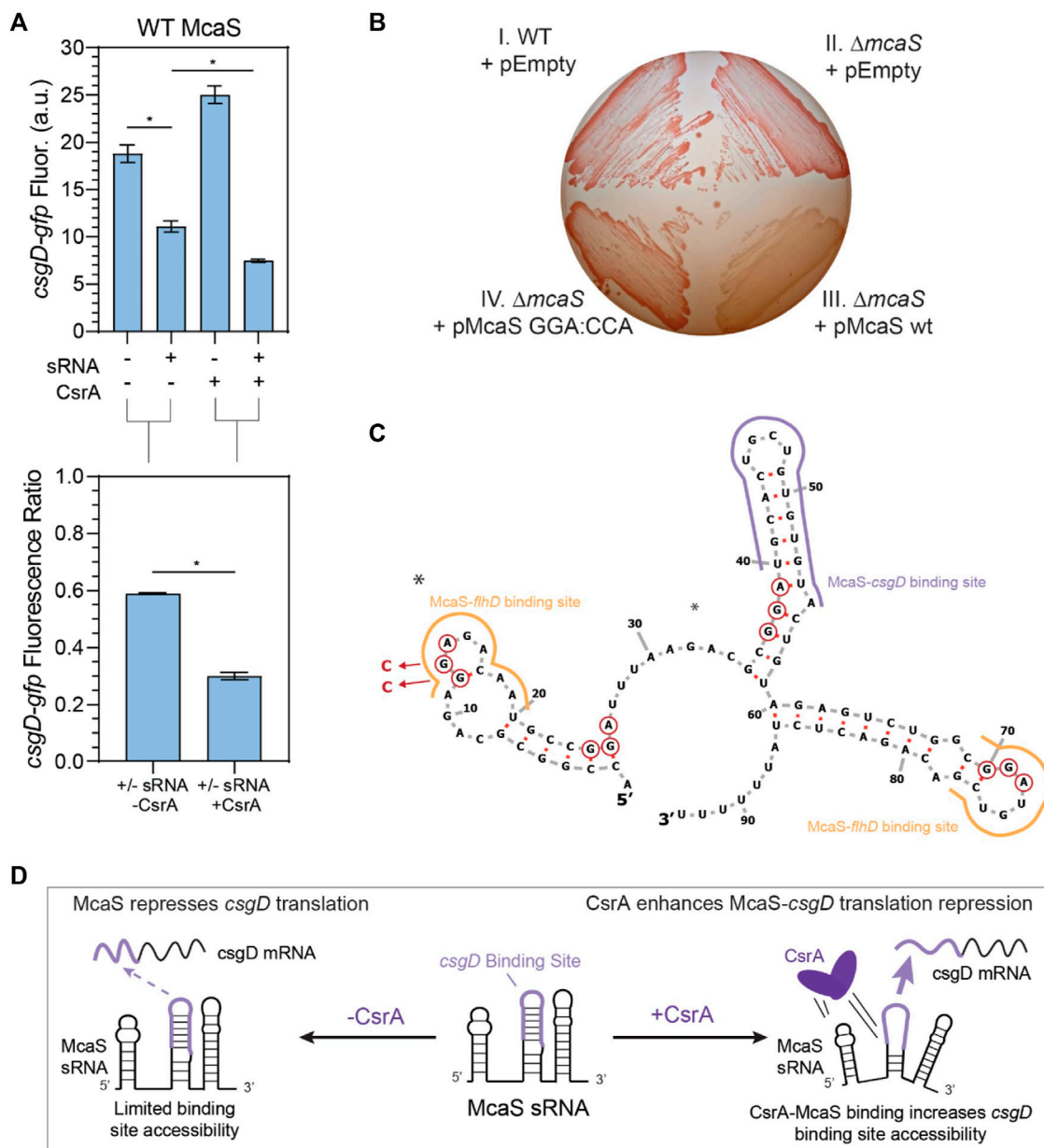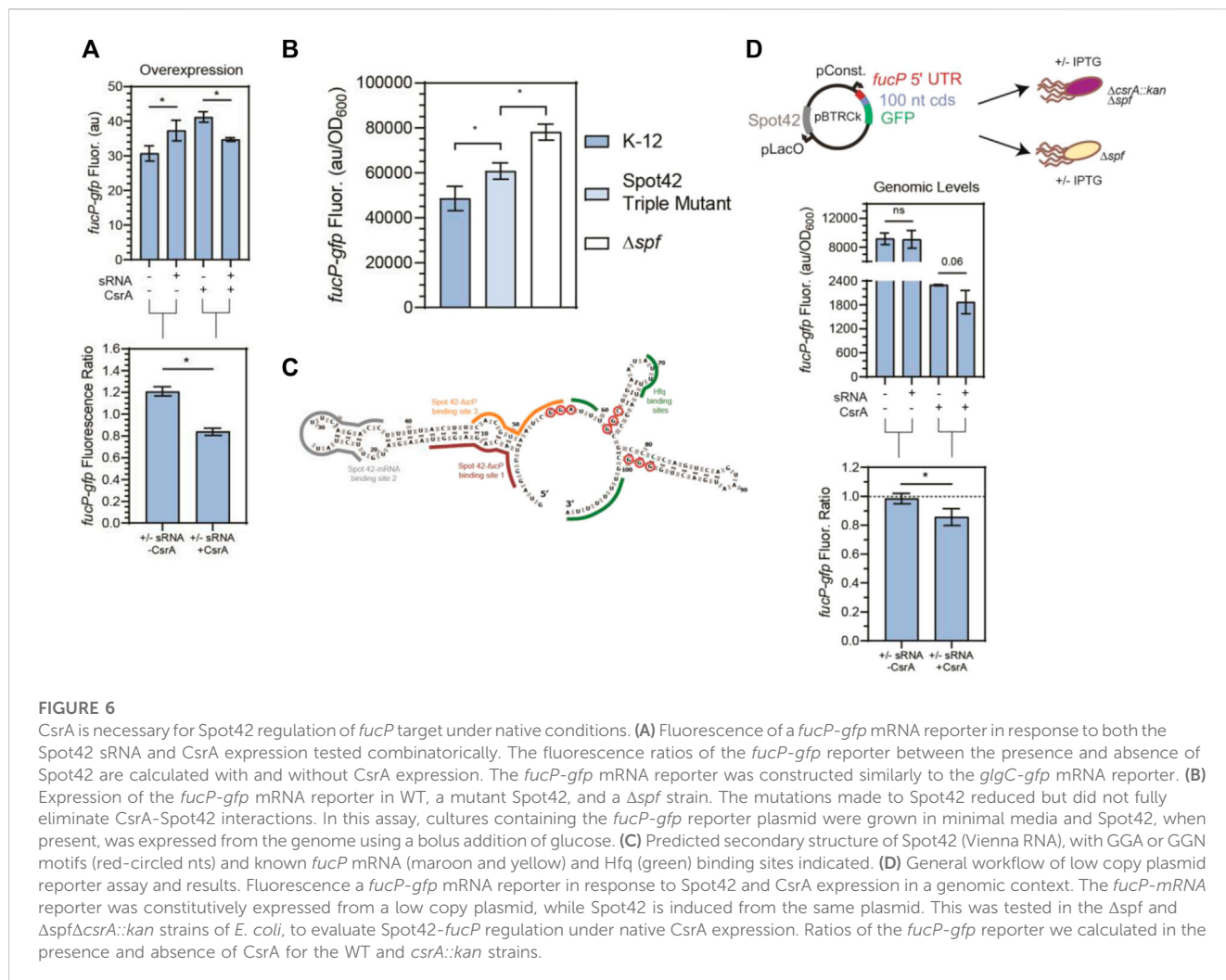
FIGURE 5
McaS-*csgD* repression is enhanced by direct CsrA interactions under native expression conditions. **(A)** Fluorescence of a *csgD-gfp* mRNA reporter in response to both the McaS sRNA and CsrA expression tested combinatorially. The fluorescence ratios of the *csgD-gfp* reporter between the presence and absence of McaS are calculated with and without CsrA expression. The *csgD-gfp* mRNA reporter was constructed similarly to the *glgC-gfp* mRNA reporter. **(B)** Effect of CsrA on McaS-csgD regulation evaluated by the Congo Red plate to measure endogenous curli expression. (Quadrant I) Wild type *E. coli* transformed with -an empty control version of a low expression plasmid (pEmpty), (II) *ΔmcaS E. coli* transformed with pEmpty (III) pMcaS wild type, and (IV) pMcaS mutant (5′-most GGA:CCA) were grown for 48 h with limited NaCl as to induce native curli expression. Plasmid-based induction of wild type McaS (1 mM IPTG) effectively repressed the *csgD* mRNA (white colonies) compared to wild type *E. coli* (dark red colonies), while mutant McaS (5′-most GGA:CCA) showed minor repression (light red colonies). **(C)** Predicted secondary structure of McaS (Vienna RNA) (Gruber et al., 2008; Lorenz et al., 2011), with GGA motifs (red-circled nts), mutations (blue arrows and nucleotides), and known *csgD* and *flhD* mRNA binding sites indicated (purple and yellow outlines, respectively). **(D)** Proposed effect of CsrA on McaS-*csgD* regulation: CsrA enhances repression by increasing mRNA-sRNA binding site accessibility.

regulatory network itself. While this work was in preparation, CsrA enhancing Spot 42-*srlA* mRNA repression was elucidated (Lai et al., 2022), setting the precedent that CsrA can remodel downstream sRNA networks. In light of these possibilities, we tested the impact of CsrA on sRNA-mRNA regulation for CyaR-*yobF*, MicL-*lpp*, Spot 42-*fucP*, Spot 42-*ascF*, SgrS-*manX* (Azam and Vanderpool, 2017), SgrS-*ptsG*, FnrS-*folX*, and McaS-*csgD*.

This subset included all sRNAs with multiple confirmed mRNA targets that we identified to interact with CsrA *in vitro* and had prior evidence of affecting CsrA *in vivo* (Table 2). It should be noted that we attempted to select the mRNA targets most sensitive to each sRNA regulator *in vivo* according to literature, if it was characterized (e.g., *ptsG* for SgrS (Bobrovskyy et al., 2019)). We excluded testing ChiX as we

FIGURE 6
CsrA is necessary for Spot42 regulation of *fucP* target under native conditions. **(A)** Fluorescence of a *fucP-gfp* mRNA reporter in response to both the Spot42 sRNA and CsrA expression tested combinatorially. The fluorescence ratios of the *fucP-gfp* reporter between the presence and absence of Spot42 are calculated with and without CsrA expression. The *fucP-gfp* mRNA reporter was constructed similarly to the *glgC-gfp* mRNA reporter. **(B)** Expression of the *fucP-gfp* mRNA reporter in WT, a mutant Spot42, and a Δ*spf* strain. The mutations made to Spot42 reduced but did not fully eliminate CsrA-Spot42 interactions. In this assay, cultures containing the *fucP-gfp* reporter plasmid were grown in minimal media and Spot42, when present, was expressed from the genome using a bolus addition of glucose. **(C)** Predicted secondary structure of Spot42 (Vienna RNA), with GGA or GGN motifs (red-circled nts) and known *fucP* mRNA (maroon and yellow) and Hfq (green) binding sites indicated. **(D)** General workflow of low copy plasmid reporter assay and results. Fluorescence a *fucP-gfp* mRNA reporter in response to Spot42 and CsrA expression in a genomic context. The *fucP-mRNA* reporter was constitutively expressed from a low copy plasmid, while Spot42 is induced from the same plasmid. This was tested in the Δ*spf* and Δspf*ΔcsrA::kan* strains of *E. coli*, to evaluate Spot42-*fucP* regulation under native CsrA expression. Ratios of the *fucP-gfp* reporter we calculated in the presence and absence of CsrA for the WT and *csrA::kan* strains.

were unsuccessful at constructing reporters for the ChiX-mRNAs *citA* and *chiP* to due to the fact the translational fusions were not fluorescent.

To evaluate the effect of CsrA on sRNA-mRNA regulation, we adapted the fluorescence assay described previously (Figure 3A) to determine the impact of sRNA-CsrA interaction on sRNA-mRNA regulation. Briefly, the *glgC* 5′ UTR was replaced with the 5′ UTR of at least one confirmed mRNA target for each sRNA and constitutively expressed in the Δ*csrBCD csrA::kan* strain. Both the sRNA and CsrA were induced on plasmids individually and concurrently to determine the impact of CsrA on sRNA-mRNA regulation.

After confirming that expected sRNA-mRNA repression was detectable for all pairs except CyaR-*yobF* (Supplementary Figure S7), we noticed that in some cases, the presence of CsrA affected the sRNA's ability to regulate its cognate mRNA target. We first observed that McaS-*csgD* repression is significantly enhanced in the presence of CsrA via our plasmid-based system. While it has been shown that McaS sponges CsrA to affect expression of CsrA targets in a CsrA-dependent manner (e.g., *pgaA*) (Jorgensen et al., 2013), there has been very little work into understanding if CsrA affects the metabolic networks that McaS itself regulates. McaS has been shown to target the *csgD* and *flhD* mRNAs, which are master

transcriptional activators of curli biogenesis and flagella synthesis (Thomason et al., 2012; Andreassen et al., 2018). From our reporter assay we observed *csgD-gfp* fluorescence is significantly lower in the presence of both McaS and CsrA, relative to McaS alone (Figure 5A, T-test *p*-value <0.05). Although *csgD-gfp* fluorescence increases upon induction of CsrA alone, this change is likely an indirect effect of expressing the global CsrA regulator. When each condition is compared to its respective CsrA null condition (+sRNA–CsrA to–sRNA–CsrA; +sRNA + CsrA to -sRNA + CsrA), repression of the *csgD* reporter significantly enhanced upon expression of McaS alongside CsrA (Figure 5A, T-test *p*-value <0.05).

To assess if direct interaction between CsrA and McaS was leading to the measured repression, a mutant Mcas sRNA was constructed with the 5′-most GGA CsrA binding site mutated (Supplementary Table S4). Using the same assay, enhanced repression in the presence of CsrA is significantly reduced when using the McaS mutant sRNA (Supplementary Figure S9A). While alleviation of repression is not fully achieved using the McaS mutant, this may be due to the fact that the second known GGA binding site for CsrA in McaS (Jorgensen et al., 2013) overlaps with the *csgD* binding site (Figure 5C) and thus not mutated. Importantly, these results suggest that CsrA is in fact remodeling the interaction between McaS and *csgD* via direct McaS-CsrA binding. This is

the first time CsrA has been observed to remodel the network of one of its sponge sRNAs. Differential McaS sRNA accumulation between the presence and absence of CsrA was confirmed to be marginal via Northern blotting analysis (Supplementary Figure S9B). Since these results were measured under sRNA overexpression, we next sought to establish if we could recapitulate these results under more relevant physiological conditions.

Enhanced McaS-*csgD* repression at physiologically relevant conditions was additionally observed by assaying curli production, a phenotype governed by *csgD* expression, on Congo Red indicator plates. In accordance with previous work (Thomason et al., 2012), endogenous expression of *csgD* produces bright red colonies in both wild type and Δ*mcaS E. coli* strains, as endogenous McaS is likely not expressed under the curli-producing conditions (Figure 5B, Panels I and II). Expression of wild type McaS from a very low copy number plasmid (~1.2 copies per cell, Material and Methods) produces opaque white colonies, indicating *csgD* repression (Figure 5B, Panel III–Lower Right). These opaque white colonies were also observed previously (Thomason et al., 2012). These data suggest that a functional McaS interaction with endogenous CsrA enhances McaS repression of *csgD* and subsequent curli formation. Importantly, expressing an McaS mutant sRNA, with a single CsrA binding site (Jorgenson et al., 2013) mutated, restores the red colony color observed when *csgD* is not repressed (Figure 5B, Panel IV–Lower Left). While these effects are mild, our results demonstrate that McaS-CsrA interactions play a role in regulating curli biosynthesis under the proper physiological conditions. While we are expressing McaS from a plasmid, due to the low copy number of the plasmid, McaS expression levels are at the same, or even lower, expression levels previously established for physiological conditions (Jorgenson et al., 2013). As a whole, this leads to the notion that the interaction between CsrA-McaS interactions may lead to downstream changes in regulatory outcomes for *csgD* regulation.

We designed this McaS mutant (5′ GGA:CCA; Supplementary Table S4) based on the hypothesis that direct CsrA binding at the 5′-most GGA in McaS is critical to enhanced *csgD* repression. Previous *in vitro* McaS-CsrA binding assays support this notion, as disrupting the 5′-most GGA of McaS impeded CsrA binding more than disrupting the GGA site that overlaps with the *csgD* binding site. Based on these data, we propose CsrA-McaS binding at the 5′-most GGA motif seeds a bridging interaction that disrupts a downstream hairpin structure containing the *csgD* binding site (Figure 5D). Such a McaS-CsrA complex could increase accessibility of the McaS binding site for *csgD* and enhance *csgD* repression. Alternatively, since McaS-CsrA binding at the 5′-most GGA motif directly overlaps a known McaS-*flhD* mRNA binding site (Figure 5C), it is plausible that McaS-CsrA interaction may bias partitioning of McaS among its mRNA targets towards *csgD* rather than *flhD*. This interaction is under further investigation.

CsrA binds Spot42 at two additional non-GGA sites and is required for Spot42 regulation of its mRNA target *fucP* under physiologically relevant conditions.

In addition to remodeling McaS-*csgD* repression, we observed that CsrA significantly impacts Spot 42-*fucP* regulation in our plasmid-based assay. Specifically, Spot 42-*fucP* repression was only observed with the *fucP-gfp* reporter when CsrA expression was induced while apparent significant *fucP* activation was detected

with the *fucP-gfp* reporter in the absence of CsrA (Figure 6A). Given that for these overexpression reporter assays (Figure 6A), CsrA was expressed on medium copy number plasmids leading to component concentrations 5–15-fold greater than native levels as previously quantified in (Sowa et al., 2017), we next evaluated if CsrA-dependent regulation could be observed under more physiologically relevant conditions.

As a tool to test biological relevance, we required a Spot42 sRNA mutant with abrogated CsrA interactions. We thus mapped the sites on the Spot42 sRNA that contributed to CsrA binding. We first conducted RNase T1 enzymatic probing of CsrA-Spot42 binding (Supplementary Figure S10A) to identify additional potential CsrA binding sites on the Spot42 sRNA, beyond the previously identified one GGA binding site that overlaps one of the RNAse E cleavage sites (Lai et al., 2022). Importantly, Spot 42 only contains one GGA CsrA binding motif, so we anticipated that additional binding sites would correspond to degenerate GGA-like sequences. From our sequencing gel, we identified protection on the 3′ region of the Spot42 sRNA, starting at nucleotide 55, in accordance with the previously identified GGA binding motif (Supplementary Figure S10A). Within the rest of the 3′ end of Spot42, we identified a GGC and GGG motif, at nucleotides 61-63 and 97-99 respectively, that showed protection in the presence of CsrA. With the GGA, GGC, and GGG motifs as guides, we ran EMSAs to evaluate the sites of Spot 42-CsrA interaction. Briefly, mutations were made to eliminate the putative binding motifs without disrupting the predicted secondary structure of the Spot42 sRNA (Supplementary Figure S10D). After testing each of the mutations in combination, we observed an ~ 1.8-fold reduction in Spot42-CsrA binding only when all three mutations were present in the sRNA (Supplementary Figures 10B, C). As such, we conclude CsrA binds Spot 42 using the established GGA site, as well as the two novel degenerate GGN sites on the 3' end of Spot42. We anticipate that a preferred interaction between Spot 42 and one binding pocket of a CsrA dimer at the GGA site likely tethers a dimer to the sRNA and allows for an additional contact to be made at a lower affinity GGN site by the other binding pocket. We expect that the single stranded GGG site is more likely bound alongside the GGA site, given its greater accessibility than the hairpin contained GGC site (Supplementary Figure S10D). Such a model has been previously proposed for CsrA-RNA binding (Mercante et al., 2009) and likely also explains CsrA repression of the *hfq* transcript, which contains only a single GGA site but presents a CsrA-occluded AGA site in *in vitro* footprinting studies (Baker et al., 2007; Leistra, Gelderman, et al., 2018). Moreover, degenerate GGA-like sequences (*e.g.,* AG-rich or GGN sequences) are thought to contribute to CsrA-RNA binding and regulation in some target mRNAs (*i.e.,* glgC, csrA, and pgaA), although these targets also contain at least two instances of the preferred GGA CsrA binding site (Mercante et al., 2009; X. Wang et al., 2005; H. Yakhnin, Yakhnin, et al., 2011).

Using this information, we designed a strain with Spot42 containing all three mutations to abrogate Spot42-CsrA interactions *in vivo*, a Δ*spf::spf_triple_*GGNs mutant (referred to as Spot42 Triple Mutant hereafter). To directly evaluate CsrA-Spot42 interactions upon the regulatory Spot42-*fucP* activity, we measured regulation of the *fucP-gfp* translational reporter expressed from a low copy number plasmid (Materials and Methods) in wild type *E. coli,* the Spot42 triple mutant strain and a Δ*spf* strain. We

induced endogenous Spot 42 transcription from the genome at an OD_{600} of 0.2 by addition of 0.2% glucose to M9 media supplemented with 0.4% glycerol and casamino acids, alleviating CRP-Spot 42 transcriptional repression, as shown in previous literature (Beisel and Storz, 2011). From this assay, we observed that the Spot42 repression of the *fucP-gfp* reporter is significantly alleviated in the Spot42 Triple Mutant expressing strain relative to the wild type Spot42 strain (Figure 6B). Additionally, to confirm that the changes in regulation we observed was due to changes interaction and not due to changes in sRNA stability, we ran a northern blot and confirmed that both the wild type and Triple Mutant Spot42 sRNAs were expressed at the same level (Supplementary Figure S14). These results point to the fact that Spot42 repression of the *fucP-gfp* is in fact partially CsrA dependent under physiologically relevant conditions. Interestingly, we could not alleviate the fucP-gfp reporter signal to that of the *Δspf* in the Spot42 Triple Mutant strain. This is likely due to network interactions other than CsrA, such as residual Hfq-driven repression of the *fucP-gfp* target by Spot42 (Beisel and Storz, 2011).

Lastly to understand if we could observe the CsrA-dependent regulation of the *fucP-gfp* reporter by Spot42 occurred under physiological conditions, we modified the reporter assay from Figure 6A such that it could be recapitulated at genomically relevant CsrA concentrations. As such, we chose to use a *Δspf* and *ΔcsrA::kanΔspf* strain of *E. coli* to replicate the plus and minus CsrA conditions and expressed Spot42 from the low copy plasmid mentioned earlier. This was chosen, as Spot42 cannot be reliably expressed from the genome in a *ΔcsrA::kan* strain (Beisel and Storz, 2011). Using this adapted assay, we observed that repression of the *fucP-gfp* reporter by Spot42 only occurred when CsrA was present. (Figure 6D). While repression of the *fucP-gfp* reporter was also observed in the absence of Spot42 when CsrA was present, *in vitro* Transcription-Translation (IVTT) assays failed to observe similar repressive effects in CsrA-only conditions (Supplementary Figure S11D). This suggests that the *in vivo* repressive effects are likely due to redundant regulation by other CsrA-regulated genes. There was no change in *fucP-gfp* reporter signal in the *ΔcsrA::kan*, regardless of Spot42 expression. Also to note, while it appears that CsrA is repressing *fucP-gfp* in the absence of Spot42 (Figure 6D – 1st and 3rd columns), this is due to the fact that the fluorescence values are normalized by growth (e.g., OD_{600}) and the -CsrA condition is derived from the *ΔcsrA::kanΔspf* strain, which exhibits poorer growth (e.g., a lower final OD_{600}). With these data in mind, we demonstrate that under physiological conditions, Spot42 repression of the *fucP-gfp* transcript is CsrA-dependent. Furthermore, IVTT results show significant repression of *fucP* by Spot42 with increasing concentrations of CsrA, supporting the fact that CsrA is needed for Spot42 regulation of *fucP* (Supplementary Figure S11D). Additionally, we observed in specific experimental conditions, such as without Hfq and CsrA regulation, Spot42 can activate translation of the fucP-gfp transcript (Supplementary Figures 11D, 12C). Spot42 can also activate the *fucP-gfp* transcript when the wild type *fucP* binding region on the Spot42 sRNA (Figure 6C–red outlined nucleotides) was mutated (Supplementary Figure S11B). Thus, there may be non-native or engineerable conditions in which *fucP* activation can occur. Lastly, while this work was being prepared a destabilizing effect of Spot42 in a *csrA* deletion strain of *E. coli* was published (Lai et al., 2022). This

work is the second known demonstration of CsrA-dependent regulation of an mRNA target via Spot42.

Discussion

In this work, we have characterized an extended overlap between the CsrA global regulatory protein and sRNA networks. Our results indicate that a much larger set of mRNA-binding sRNAs bind CsrA *in vitro* (Figure 2; Table 2) and that sRNA-mRNA regulation can be impacted by CsrA *in vivo.* Importantly, our data support the notion that CsrA-sRNA interactions result in different post-transcriptional regulatory schemes and have selective impacts in the mRNA target network of the sRNA.

Consistent with the notion of sRNAs acting as sponges that sequester CsrA *in vivo*, we have also identified FnrS and SgrS as two novel sRNA that sequester CsrA when present at a sufficient intracellular concentration (Figure 3). Importantly, we observed that under physiological conditions, SgrS can act as a CsrA sponge (Supplementary Figure S13), specifically when grown in LB the presence of *a*-methyl glucoside (Wadler and Vanderpool, 2007). We attempted to establish sponging activity for FnrS utilizing anaerobic conditions previously established for genomic FnrS expression (Durand and Storz, 2010), but could not replicate and confirmed previously observed differential FnrS expression (Boysen et al., 2010; Durand and Storz, 2010) and could not evaluate sponging activity. These results emphasize the condition-dependence of these CsrA sRNA sponges, and that CsrA may only be sponged by specific sRNAs under very specific environmental conditions. It is plausible that there are additional growth conditions in which these sRNAs play a larger role in sequestering and titrating CsrA, which is an ongoing investigation for the field.

Beyond the sequestration mechanism, our data support novel influence of the global CsrA regulatory protein on the downstream regulatory roles of sRNAs under physiologically relevant conditions: two examples in this work are the enhancement of McaS-*csgD* repression (Figure 5) and the CsrA-dependent repression of *fucP* by Spot42 (Figure 6), involving new regions of Spot 42-CsrA interactions that include non-canonical degenerate GGA sites, which have not been widely reported. From our *in vivo* reporter assays, we observed that expressing McaS and CsrA simultaneously led to enhanced *csgD* repression, relative to *csgD* repression when only expressing McaS (Figure 5A). Furthermore, we demonstrate this regulatory pattern is consistent under physiologically relevant concentrations and has observable phenotypic outputs by assaying curli production (Figure 5B). While McaS has been previously shown to interact with CsrA (Jorgensen et al., 2013), McaS was implicated as a sRNA sponge of CsrA. Our work demonstrates a new role of CsrA in the context of remodeling the metabolic network of McaS, as shown at least by the case of McaS-*csgD* regulation. We can begin to deduce the native context in which CsrA may remodel such sRNA-mRNA interactions by considering known expression conditions and activity for each regulator (Supplementary Table S2). For example, high McaS expression coupled with low CsrA availability (in early and mid-stationary phase), may not yield any observable effects on the mRNA target. But McaS expression under high CsrA availability (in late stationary phase) may demonstrate

enhanced McaS-*csgD* repression by CsrA, as these conditions allow McaS to effectively compete for CsrA sequestration.

Beyond the role of CsrA on the regulatory roles of McaS and Spot42, we observed that MicL-*lpp* repression is significantly impeded in the presence of CsrA (Supplementary Figure S8); MicL is another well-characterized sRNAs known to be the key regulatory sRNA in outer membrane protein synthesis and can even affect Sigma E transcription factor activity (Guo et al., 2014). Notably, the most likely predicted MicL-CsrA binding region overlaps the known MicL-*lpp* binding site (Supplementary Figure S8E. As such, we evaluated the hypothesis that MicL-CsrA binding directly occludes MicL-*lpp* binding *in vitro* and we observed that the presence of CsrA decreased MicL-*lpp* complex formation approximately two-fold in EMSA analysis (Supplementary Figure S8D). However, given the small effect size *in vivo* and overall limited extent of MicL-*lpp* binding *in vitro*, these observations require further work to confirm direct impact of CsrA on MicL-*lpp* regulation.

In the case of Spot42, the impact of CsrA on mRNA regulation varies. In this work, CsrA is required for Spot42-*fucP* regulation (Figure 6) but does not impact *ascF* repression (Supplementary Figure S7), despite *ascF* being another confirmed target of Spot42 (Beisel et al., 2012). While this work was in preparation, CsrA-Spot42 binding was shown to enhance Spot42-*srlA* repression *in vivo* (Lai et al., 2022). Our observations that Spot42 requires CsrA to repress *fucP* is the second known example of this form of CsrA-dependent sRNA-mRNA regulation and opens the door towards new ways by which CsrA can remodel the global post-transcriptional landscape, as well as the interplay between CsrA and RNAse E networks.

Previously, Spot42 has been shown to be destabilized in a *csrA* mutant strain *in vivo* (Lai et al., 2022). Interestingly, we observed that CsrA affects Spot42 regulation of *fucP* (Figure 6) and *srlA* (Lai et al., 2022), but not of its other mRNA target *ascF* (Supplementary Figure S7). Our observations on the requirement of CsrA for the selective repression of some Spot42 targets (*i.e., fucP*) by Spot42 are consistent with a hypothesis in which CsrA affects availability of specific target binding sites within the Spot42 sRNA in addition to its general stability. Further support for this hypothesis stems from the observation that Spot42 has non-overlapping binding sites for *ascF* and *galK* mRNA targets but not for *srlA* and *fucP* (Beisel et al., 2012). Collectively, this data suggests that CsrA can affect sRNA-mRNA regulation in a selective fashion. Furthermore, given that *In Vitro* Transcription and Translation (IVTT) assays ruled out the possibility of CsrA directly binding the *fucP* in these interactions (Supplementary Figures S11D, E) we propose that the general model for CsrA impacting sRNA-mRNA regulation differs from that of Hfq and ProQ in that a CsrA dimer is not anticipated to bind two different RNA molecules at each of its binding faces and seed annealing. Rather, we presume that a CsrA dimer binds at two sites within a single sRNA to directly occlude sRNA-mRNA binding or alter sRNA-mRNA binding availability at a neighboring region. As such, our results show that CsrA interacts with Spot42 via binding at the previously known GGA site, as well as degenerate GGNs at the 3' end of the sRNA (Figure 6B;Supplementary Figure S11A). This model is consistent with current understanding of CsrA-mRNA regulatory mechanisms (Mercante et al., 2009; Romeo and Babitzke, 2018).

Interestingly, we observed a bi-directional response of Spot42-*fucP* regulation in the presence or absence of overexpressed CsrA in our initial overexpression *in vivo* reporter assays (Figure 6A). In the absence of CsrA, the *fucP-gfp* reporter was activated when co-expressed with Spot42, but in the presence of CsrA, *fucP-gfp* signal was repressed (Figure 6A). While not initially observed in a genomic context (Figure 6B), upon mutating the canonical Spot42-*fucP* binding site on the *fucP-gfp* reporter, we observed the same CsrA-dependent toggling effect at genomic levels (Supplementary Figure S11B). Moreover, our IVTT assays also showed the bidirectional response upon adding Spot42 sRNA and titration of CsrA into these reactions (Supplementary Figure S11D). These results lay the foundation of the possibility that CsrA could be used as a synthetic bi-directional regulator to construct toggle switches. Previously, post-transcriptional circuits that leverage natively expressed proteins with engineered RNAs are some of the most powerful in synthetic biology (Na et al., 2013; Noh et al., 2017).

Our work here uncovered several novel interactions of sRNAs binding both CsrA and Hfq in ternary complexes; such binding has been previously reported for McaS (Jorgensen et al., 2013) and observed for ChiX and DsrA (personal communication, Dr. Sarah Woodson's lab). We report new CsrA-Hfq ternary complexes also with SgrS, FnrS, CyaR, GadY, MicL, RnpB, and GlmZ (Figure 2; Supplementary Figure S2). Several lines of evidence support the hypothesis that these ternary complexes are RNA-mediated, rather than purely dependent on protein-protein interaction. For instance, the sRNAs Spot42, DsrA, GcvB, and SibD bind Hfq but do not show CsrA-sRNA-Hfq ternary complexes. This contrasts with what would be expected if CsrA and Hfq-associated on a protein-only basis. Additionally, it was recently shown that in *E. coli*, CsrA co-purifies with Hfq in an RNA-dependent manner (Caillet et al., 2019). Similarly, a modified ChIP-seq study in *Pseudomonas aeruginosa* reports approximately 180 nascent transcripts that contain mostly non-overlapping enrichment peaks for both RsmA (a CsrA homolog) and Hfq (out of 560 total RsmA enrichment peaks) (Gebhardt et al., 2020). These nascent transcripts are likely simultaneously bound by both regulators, as most of these peaks do not directly overlap. Given the ternary CsrA-sRNA-complexes we observed *in vitro* (Figure 2) and the high throughput studies mentioned above (Caillet et al., 2019; Gebhardt et al., 2020), the possibility of sRNA-mediated CsrA-sRNA-Hfq ternary complexes forming in our *in vivo* assays, and, more broadly, endogenously throughout *E. coli* post-transcriptional regulation seems likely. The bulky ternary complexes could have inhibited *in vivo* detection of some of our CsrA-sRNA pairs in the context of our GFP-complementation assays (Supplementary Figure S4).

Overall, from a Csr systems perspective, remodeled sRNA-mRNA regulation allows inference of a new paradigm for understanding the scope of Csr network regulation. Prior omics studies of the Csr system imply wide-spread effects of CsrA deletion, more than what can be accounted for by the number of confirmed mRNA targets (Potts et al., 2017; Sowa et al., 2017). While CsrA regulation of transcription factors and sigma factors, such as *nhaR, sdiA, rpoE*, and *iraD* (an anti-adaptor protein that inhibits RpoS degradation) (A Pannuri et al., 2012; Park et al., 2017; H. Yakhnin et al., 2017; H. Yakhnin, Baker, et al., 2011), begin to explain these effects, crosstalk between CsrA and post-transcriptional sRNA regulators is likely to contribute. However, these crosstalk effects are difficult to extract from high throughput RNA-seq and proteomics studies because the effects of CsrA remodeling sRNA

regulatory networks are likely, as we propose, target specific. We anticipate that an *in vivo* role for CsrA in remodeling sRNA-mRNA regulation extends beyond the examples highlighted here. While precise mechanistic characterization is still needed, CsrA-remodeled sRNA-mRNA regulatory interactions may serve as templates for better understanding how global RNA-binding proteins extend their regulatory reach in cells. Even more broadly, this work sets the stage to investigate the full physiological impacts of the overlapping network interactions between CsrA and other global RBP networks.

Materials and Methods

Bacterial strains and growth conditions

All *E. coli* strains used in experiments are derivatives of K-12 MG1655 and are described in Supplementary Tables S1–S4. DH5α (NEB) and BL21 (DE3) (NEB) *E. coli* strains were used for cloning and protein purification, respectively. Routine cultures were performed in LB medium (Miller) (BD Biosciences) with 50 μg/mL kanamycin and/or 100 μg/mL carbenicillin as required. Starter cultures were grown from single colonies overnight in 5 mL LB (test tubes) at 37°C with 200 rpm orbital shaking. Cultures were diluted 1:100 in LB media for fluorescence assays and protein purification except where noted otherwise. Final concentrations of 1 mM isopropyl ß-D-1-thiogalactopyranoside (IPTG) and 100 ng/mL anhydrotetracycline (ATc) were used in cultures to induce plasmid expression. Congo red plate assays were performed on agar plates containing LB medium without salt (10 g/L yeast extract, 5 g/L tryptone, 0 g/L NaCl), 40 μg/mL Congo red dye, 20 μg/mL Coomassie Brillant Blue G 250 dye, 50 μg/mL kanamycin, and 1 mM IPTG (Bak et al., 2015). Kanamycin resistance cassettes were cured from *sRNA::kan* deletion strains (Supplementary Tables S1–S4) and confirmed by colony PCR prior to use as previously described (Cherepanov and Wackernagel, 1995; Datsenko and Wanner, 2000). Genomic expression conditions for SgrS and FnrS were adapted directly from previous established protocols for expressing SgrS (Wadler and Vanderpool, 2007 *PNAS*) and FnrS (Durand and Storz, 2010 *Mol. Microbiol.*).

Plasmid construction

Plasmids used in this study are documented in Supplementary Tables S1–S4. All plasmids were constructed by Gibson assembly or purchased from Genscript. Oligonucleotide primers for Gibson assembly were designed using the NEBuilder 2.0 web tool and are included in Supplementary Tables S2–S6. DNA oligonucleotides and double stranded DNA fragments (GBlocks) were purchased from Integrated DNA Technologies. Plasmids were verified by Sanger sequencing (University of Texas GSAF core). Details on cloning methods used for construction of pTriFC plasmids, pHL600 pLacO-*sRNA* pTetO-*csrA* plasmids, pHL1756 5′UTR-*gfp* reporter plasmids, pBTRK-pLacO-sRNA plasmids, and pBTRK-pLacO-*fucP-gfp* (CmR) plasmids are included in Supplementary Material. It should be noted that the pBTRK-pTrc-Empty plasmid, a generous gift from the lab of Dr. Brian Pfleger that contains a very low copy number pBBR-1 origin (~1-3 copies per cell) (Youngquist et al., 2013; Hernández Lozada et al., 2018), was used as a parent plasmid for the pBTRK-pLacO plasmids constructed in this work.

Strain construction

A previously-demonstrated CRISPR-cas9 genome modification protocol was used to construct Δ*spf* and GGA:GCA mutant *spf* K-12 MG1655 strains (Mehrer et al., 2018). It should be noted that the *spf* gene encodes the Spot 42 sRNA. This approach uses a two-plasmid system to achieve genomic deletion or insertion. The first plasmid, a generous gift from the lab of Dr. Brian Pfleger, provides kanamycin-resistant guide RNA (gRNA) expression under the constitutive J23119 promoter and is termed pgRNA. The second plasmid, pMP11, is a temperature sensitive, carbenicillin-resistant plasmid that contains 1) wild type cas9 from *Streptococcus pyogenes* under the J23119 constitutive promoter, 2) λ-red recombinase under the pBAD promoter, and 3) a gRNA specific to the pgRNA plasmid to enable its removal under a pTeto promoter.

A gRNA for deletion of the *spf* gene was designed using the CRISPR gRNA Design webtool from Atum (atum.bio). This sequence was cloned into the gRNA plasmid by Gibson Assembly (Supplementary Tables S2–S6). Additionally, a dsDNA gBlock was designed to contain the desired *spf* deletion (here, the last 7 nt of the sRNA) or mutation sequence plus 500 base pairs of sequence homologous to the genome upstream and downstream of the edit site. To avoid gRNA-directed cleavage of the dsDNA homology GBlock, we targeted the gRNA to the CDS of a protein-coding gene, *yihA*, 150 nucleotides 3′ of *spf*. Synonymous codon mutations were made to the gRNA binding site in the dsDNA homology GBlock to protect it from pgRNA-directed cleavage. As a result, the 500 nucleotide homology regions were defined to be 500 nucleotides 5′ of *spf* and 3′ of *yihA* (Sequence in Supplementary Tables S2–S6).

K-12 MG1655 *E. coli* containing the pMP11 plasmid was grown in 5 mL of LB overnight to saturation. The overnight culture was diluted 1:100 in 50 mL of SOB media (BD Biosciences) and grown at 30°C until an OD_{600} of 0.2. The *?*-red genes were then induced by addition of 1% w/v L-arabinose. At an OD_{600} of 0.4–0.6, the culture was made electrocompetent according to common lab procedures. 50 ng of the gRNA plasmid and 25–50 ng of the dsDNA homology block was added to a single aliquot of electrocompetent cells, and subsequently transformed. Transformants were recovered in 1 mL of SOB media at 30 °C for at least 3 hours, plated onto LB agar plates containing kanamycin and carbenicillin, and grown at 30 °C. Gene deletions were confirmed via colony PCR (Supplementary Tables S2–S6) and sanger sequencing of the purified pcr fragment.

Upon verification of the *spf* deletion or mutation, the gRNA plasmid was cured by growing a single colony in 5 mL of LB containing carbenicillin and 0.2 ng/mL aTc overnight at 30 °C. Single colonies were of this culture were generated and streaked on carbenicillin *versus* kanamycin and carbenicillin LB agar plates to confirm pgRNA plasmid removal. The pMP11 plasmid was then cured by patching successful colonies onto LB agar only plates and growing overnight at 42°C. Removal of pMP11 was verified by streaking on LB agar only *versus* LB agar plates with carbenicillin.

Analysis of csr RNAseq data

RNA sequencing and downstream data analysis was previously performed for *csrA::kan* mutant, Δ*csrB* Δ*csrC*, and wild type (WT) K-12 MG1655 *E. coli* strains before and after glucose deprivation in

M9 minimal media (Sowa et al., 2017). Briefly, biological triplicate cultures were grown to an OD_{600} of 0.6 in M9 media with 0.2% glucose before centrifugation and resuspension in fresh M9 media lacking glucose. Samples were taken 10 min and 0 min prior and 30 min, 60 min, 180 min, and 300 min after glucose starvation. Aligned, counted reads from the previous work were reanalyzed by DESeq2 to include sRNAs and tRNAs (rRNA read counts were still excluded from analysis). As done in the prior work, all samples of the $\Delta csrB\ \Delta csrC$ strain collected 300 min post stress were excluded from further analysis due to large variation amongst the replicas. Additionally, principal component analysis identified one sample, a replica of the of the $\Delta csrB\ \Delta csrC$ strain collected at time 0, that clustered far from the rest of the data. Data from this sample were also excluded from further analysis. Strain and time factors were paired in order to identify differentially expressed genes between the WT and csrA::kan strains and the WT and $\Delta csrB\ \Delta csrC$ strains at each time point. sRNAs differentially expressed (log2 fold change >1 or < −1 and Wald test P-adjusted <0.05) between the WT and $\Delta csrB\ \Delta csrC$ strains at two time points or more were considered as potentially interacting with the Csr system and selected for further study (Supplementary Tables S3–S7). It should be noted that by these criteria, no sRNAs were differentially expressed between the WT and csrA::kan strains. As levels of free CsrA are likely increased in the $\Delta csrB\ \Delta csrC$ strain (Sowa et al., 2017), we considered differential expression between the WT and $\Delta csrB\ \Delta csrC$ strains to indicate sRNAs likely impacted by CsrA.

Thermodynamic prediction of sRNA binding sites

The biophysical model estimates the free energy of CsrA binding to pairs of 5 nucleotide potential binding sites within an RNA of interest based on RNA sequence, structure, and inter-site spacing. Based on these predictions, we analyzed the 15 most likely, i.e., lowest free energy, CsrA-RNA binding conformations, to identify putative CsrA-RNA binding regions. Previously, we confirmed the utility of this model for correctly predicting CsrA binding sites for 6 mRNAs of 8 total that have documented CsrA footprints. Within this subset, the model also successfully captured CsrA footprints for 3 mRNAs that lack the preferred GGA motif. When the model was run for sRNAs, predicted CsrA binding sites overlap GGA motifs found within the sRNA sequences (Supplementary Tables S3, S4). They also highlight non-GGA containing regions that may contribute, albeit likely transiently, to sRNA-CsrA recognition and binding in these sRNAs. Importantly, predicted sRNA-CsrA binding sites in the FnrS and MicL sRNAs, which lack GGA motifs, highlight a distinct region in each sRNA that contains a bulk of the predicted binding sites. CsrA-sRNA binding sites were predicted as previously done for mRNAs (Leistra et al., 2018) and are further explained in the Supplementary Material.

Protein purification

CsrA was purified as previously published (Dubey et al., 2005) with minor modifications, as described in the Supplementary Material. Hfq was purified according to published methods (Santiago-Frangos et al., 2016) and generously gifted to us by the lab of Dr. Sarah Woodson.

In vitro electrophoretic mobility shift assays

Primers were designed to amplify sRNAs (Supplementary Tables S2–S6) with an upstream T7 promoter from genomic K-12 MG1655 DNA (wild type sRNA sequences) or previously constructed plasmids (mutant sRNA sequences). Forward primers were designed to contain four random nucleotides (GACT) upstream of the promoter sequence (TAATACGACTCACTATAGGGAGA). PCR product sizes were verified on a 1% agarose gel prior to PCR clean up (DNA Clean and Concentrator-5, Zymo). A DNA fragment for transcription of lpp (lpp sequence preceded by aforementioned T7 transcription-enabling sequence) was manufactured by Integrated DNA Technologies (Supplementary Tables S2–S6).

Lpp was in vitro transcribed using the MEGA Script IVT Kit (Thermo Fisher Scientific) according to manufacturer instructions (with incubation time extended to 6 h as recommended for <500bp RNA products). sRNAs were transcribed with modifications to enable internal P-32 labeling. Specifically, 1.5 μL UTP [α-32P] (3000 Ci/mmol 10 mCi/mL, 500 μCi, PerkinElmer) was used to replace equivalent unlabeled UTP from the MEGA Script IVT kit. Following MEGA Script T7 DNase digestion, RNA recovery was performed using RNA Clean and Concentrator-5 (Zymo Research) according to manufacturer instructions. RNA samples were re-suspended in 20 μL of nuclease-free water following recovery and, for sRNAs only, free NTPs removed using DTR Gel Filtration Cartridges (EdgeBio) following manufacturer instructions. RNA concentration was measured via spectrophotometry, and, in the case of lpp, transcript quality validated on an 8% urea gel, run at 100 V for 3 h, and stained with Sybr Green II (Thermo Fisher Scientific).

EMSAs were performed largely according to the TBE CsrA-RNA gel shift protocol detailed in (A. V Yakhnin et al., 2012), with modifications to support the use of a different CsrA dilution buffer (Dubey et al., 2005). Twelve μL binding reactions were comprised of 10 nM denatured sRNA (3 min at 85°C), 1 μL 10X CsrA binding buffer (100 mM Tris-HCl pH 7.5, 100 mM $MgCl_2$, 1 M KCl), 4 μL CsrA dilution buffer (same as CsrA storage buffer: 10 mM Tris-HCl, 100 mM KCl, 10 mM $MgCl_2$, and 25% glycerol, pH 7.0), 11% glycerol, 20 mM DTT, 333 U/mL RNase Inhibitor, Murine (NEB), 1.5 μg/μL yeast total RNA, 0–6 μM CsrA, and 0, 0.375, 1.5, or 3 μM Hfq. These concentrations of Hfq were selected to mimic the expected relative in vivo expression ratios of CsrA to Hfq based on estimations of their in vivo concentrations: 0.4–10 μM hexameric Hfq per cell (Kajitani et al., 1994; Moon and Gottesman, 2011; Wagner, 2013) and 6–17 μM dimeric CsrA (Romeo et al., 2013). Importantly, each reaction contained an excess of total yeast RNA (Thermo Scientific) to exclude results due to non-specific binding. For these experiments, radiolabeled sRNAs (10 nM) were incubated with 3 μM or 6 μM concentrations of CsrA at 37°C for 30 min prior to loading and running on a 10% non-denaturing polyacrylamide gel (A. V Yakhnin et al., 2012) with 0.5X TBE running buffer (IBI Scientific, 10x composition: 89 mM Tris, 89 mM Boric Acid, 2 mM EDTA) at 170 V between 5 h and overnight (depending on sRNA) at 4°C. These concentrations of CsrA represent Protein:sRNA ratios of 300:1 and 600:1, respectively. These ratios were selected to screen for CsrA-sRNA binding based on CsrA binding affinities reported for Spot 42, GadY,

GcvB, and MicL, interactions presumed to be relevant *in vivo* based on significant enrichment in CsrA CLIP-seq data (Potts et al., 2017). Briefly, these previous *in vitro* binding assays employed molar ratios of CsrA:sRNA ranging from 50:1 to 2,000:1 (5 nM CsrA:0.1 nM sRNA to 200 nM CsrA:0.1 nM sRNA) and determined dissociation constants in the range of 100:1 to 660:1 CsrA:sRNA (10 nM CsrA: 0.1 nM sRNA to 66 nM CsrA:0.1 nM sRNA). While our assays scale up the total molar amount of each component, they test CsrA-sRNA binding at molar ratios of 300:1 and 600:1 CsrA:sRNA. These ratios are within the range of CsrA-sRNA binding affinity presumed to be physiologically relevant in (Potts et al., 2017). Additionally, all binding assays are performed in large excess of yeast total RNA (88 ng/μL, as in (A. V Yakhnin et al., 2012)) to inhibit non-specific association of CsrA to labeled sRNAs.

Gel exposure on a bioWORLD bioExposure cassette was phosphor-imaged at 1000 V using Typhoon FLA 700 (GE Health Life Science).

MicL-*lpp*-CsrA EMSA was performed with slight modifications. Larger reaction volumes (15 uL) were used to accommodate addition of the *lpp* 5' UTR (80 or 240 nM final concentration) and relative molar amounts of sRNA and CsrA equivalent with the gels described above were included (8 nM denatured sRNA and 0, 2.4, or 4.8 μM CsrA). All other components of the binding reaction were scaled appropriately.

Tri-fluorescence complementation assays

Fluorescence complementation assays to detect RNA-protein binding *in vivo* were conducted as previously described, with modifications as described in the Supplementary Material.

GFP fluorescence quantification

sRNA-CsrA sponge activity

Plasmid-based screening of sRNA-CsrA sponge activity was inspired by a previous study (Adamson and Lim, 2013; Leistra et al., 2017). Here the plasmid encoding inducible CsrA and sRNA expression was altered to control expression of the sRNA with the stronger pLacO promoter (rather than a pTetO promoter used in the previous study). Expression of CsrA was controlled with the weaker pTetO promoter (rather than the pLacO promoter used in the previous study). The modified plasmid system was expressed in a K-12 MG1655 *E. coli* strain deleted for the Csr system (ΔcsrA ΔcsrB ΔcsrC ΔcsrD) and lacking the *pgaABCD* and *glgCAP* operons, as before (Adamson and Lim, 2013; Leistra et al., 2017). Single colonies of ΔcsrA ΔcsrB ΔcsrC ΔcsrD ΔpgaABDC ΔglgCAP lacI$_q$ K-12 MG1655 *E. coli* cells (Adamson and Lim, 2013) harboring pHL600 pLacO-sRNA pTetO-*csrA* and pHL1756 *glgC-gfp* plasmids were grown up overnight in 5 mL cultures. Biological triplicate overnights were seeded in 30 mL of LB (1:100 dilution, in flasks) with 100 ng/mL aTc to induce CsrA expression. After growth to an OD$_{600}$ of 0.4 (~3 h), each culture was split in half and 1 mM IPTG was added to one 15 mL volume to induce sRNA expression. Green fluorescence was measured with a BD FACSCalibur flow cytometer (~25,000 cells per sample) after 2 additional hours of growth to an OD$_{600}$ of 1.5–2.0. Fold

change in median green fluorescence between + sRNA and–sRNA conditions was determined for each biological replicate and averaged (n = 3). Two-tailed heteroscedastic t-tests were used to assess whether fold change in *glgC-gfp* fluorescence upon sRNA induction was significantly increased relative to that of the random RNA (p-value <0.05). The assay was similarly conducted in the absence of induced CsrA expression, with the exception that each biological replicate starter culture was seeded in 15 mL of LB in technical duplicate. Once cultures reached an OD$_{600}$ of 0.4, sRNA expression was induced in half of the cultures with 1 mM IPTG such that a +sRNA and–sRNA culture was obtained for each biological replicate. Green fluorescence was measured at the same conditions. It should be noted that in the absence of CsrA induction, cultures grew more slowly: 4.5 h to OD$_{600}$ 0.4 and approximately 4 additional hours to OD$_{600}$ 1.5.

Impact of CsrA on sRNA-mRNA regulation

The same *E. coli* strain and plasmid system were used to assay the impact of CsrA on sRNA-mRNA regulatory pairs. Here, the 5′ UTRs of mRNAs regulated by sRNAs were used as translational GFP fusion reporters, as is typically done to test sRNA-mRNA interactions *in vivo* (Beisel and Storz, 2011; Bobrovskyy et al., 2019; Miyakoshi et al., 2019). Briefly, 5′ UTRs were defined as the region between the transcription start site and the mRNA start codon. This region, plus the first 100 nucleotides of mRNA coding sequence, was cloned in frame with *gfp* as previously published (Sowa et al., 2017; Leistra, Gelderman, et al., 2018). For simplicity, the 5′ UTR term is used to refer to the whole region cloned in frame with *gfp*. For mRNAs that code for membrane proteins, only the first 10 nucleotides of coding sequence were included in the reporter to minimize the impact highly hydrophobic amino acids might have on proper GFP folding and function (Supplementary Tables S1–S4 for full sequences tested). This length of sequence was chosen to reflect the range of coding sequence that is occluded upon ribosome-RBS binding (Espah Borujeni et al., 2017). However, if the sRNA binding site is or overlaps 3′ of the first 10 coding sequence nucleotides, the 5′ UTR was extended to include 10 nucleotides of coding sequence nucleotides beyond the 3′ edge of the sRNA binding region. For mRNAs in which the transcription start site is not known, the 100 nucleotides preceding the start codon was designated as the 5' UTR (Sowa et al., 2017).

Single *E. coli* colonies expressing a pHL600 pLacO-sRNA pTetO-*csrA* plasmid and a corresponding pHL1756 5′ UTR-*gfp* plasmid were grown in 5 mL LB overnight to saturation. Saturated starter cultures were diluted 1:100 into 15 mL of LB (in flasks) four times. After growth to an OD$_{600}$ of 0.2–0.3, sRNA and CsrA expression was induced (1 mM IPTG and 100 ng/mL ATc, respectively) such that the following four conditions were obtained for each biological replicate: sRNA–CsrA; +sRNA–CsrA; –sRNA + CsrA; +sRNA + CsrA. Green fluorescence was measured with a BD FACSCalibur flow cytometer at several time points after induction. Fold change in median fluorescence value was calculated between induction conditions and averaged for biological replicates (n = 3). Paired two-tailed t-tests (p-value <0.05) determined whether changes in fluorescence were significant. Heteroscedastic two-tailed t-tests (p-value <0.05) were used to compare fluorescence fold changes measured for wild-type and mutant versions of the Spot 42 sRNA and *fucP-gfp* 5' UTR reporter.

RNA extraction

Total RNA was extracted from cultures tested in GFP fluorescence assays by the TRIzol manufacturer protocol (Thermo Fisher Scientific) with a few modifications as described in the Supplementary Material.

Northern blot analysis

Northern blotting was performed as previously reported (Cho et al., 2014), with a few modifications as described in the Supplementary Material.

Enzymatic probing of CsrA interaction with Spot42 sRNA

RNase T1 probing of Spot42 was performed as previously described (Salvail et al., 2010) with a few modifications described in the Supplementary Material.

Western blot analysis

To quantify CsrA expression levels in the GFP fluorescence assays, 9–10 mL of the 15 mL culture tested was pelleted by 10 min of centrifugation at 4000 rpm and 4°C. The supernatant was discarded and the pellet was flash frozen using liquid nitrogen and stored at −80°C for future use. Pellets were lysed and western blots conducted as described in the Supplementary Material.

In vitro transcription and translation assays

Coupled transcription-translation assays were carried out with the PURExpress kit (New England BioLabs) as described in (Lukasiewicz and Contreras, 2020) with a few modifications described in the Supplementary Material.

qRT-PCR quantification of sRNA effects on CsrA mRNA targets

Potential sRNA sponge or sequestration activity for endogenous CsrA and its mRNA target network was tested in K-12 MG1655 strains. CsrB, McaS, or SgrS sRNAs were cloned into the low copy number pBTRK-pLacO-Empty parent plasmid and expressed in a corresponding sRNA deletion strain ($\Delta csrB\Delta csrC$, $\Delta mcaS$, or $\Delta sgrS$ K-12 MG1655, respectively). Single colonies of these strains were grown up overnight in 5 mL cultures. Biological triplicate overnights were seeded in 30 mL of LB (1:100 dilution, in flasks). After growth to an OD_{600} of 0.2, each culture was split in half and 1 mM IPTG (final concentration) was added to one 15 mL volume to induce sRNA expression. Thirty minutes later, at an OD_{600} of 0.6, 5 mL volumes of all samples were harvested by centrifugation. RNA extraction was performed as described above. After verifying RNA quality, 10 μg of RNA was treated with DNase (DNAse I RNas-free, NEB) for 10–15 min at 37°C. RNA was immediately re-purified with spin columns (RNA Clean and Concentrator-5 kit, Zymo Research) and concentration determined by nanodrop.

Abundance of the following RNAs was assessed by qRT-PCT in each sample: CsrA target mRNAs *glgC* and *pgaA;* non-target mRNA *phoB;* the sRNA induced, i.e., CsrB, SgrS, or McaS; and housekeeping reference RNAs *secA* and 16s. The *secA* mRNA and the 16s rRNA were both employed as housekeeping references as the endogenous mRNAs in question were much lower in abundance than the standard 16s rRNA reference.

Additionally, *secA* has been previously used a housekeeping reference target in prior Csr study (Butz et al., 2019). Primers for qRT-PCR reactions were designed with the IDT PrimerQuest tool, specifying dye-based qPCR quantification. All primer pairs yielded amplicons of 75–125 nucleotides. Primer efficiencies were determined for each pair to be 90%–105% across a 10^4-fold range of RNA concentrations (0.005–5.0 ng or 0.05–50 ng RNA). It should be noted that 50 ng of RNA was needed to detect mRNAs with an approximate threshold cycle (C_T) value of 20, while only 0.005 ng was needed to detect sRNAs and the 16s rRNA at the same approximate C_T value.

Biological triplicate RNA samples were tested in technical triplicate for each RNA target (i.e., each primer pair). All qRT-PCR reactions were performed with the Luna universal One-Step RT-qPCR kit (E3005 NEB) according to manufacturer protocol with a few modifications. Reactions were prepared as follows in 384 well plates (MicroAmp Optical 184-Well Reaction Plate, Thermofisher): 5 μL Luna one-step reaction mix, 0.5 μL Luna RT mix, 0.4 μL of 10 μM forward primer, 0.4 μL of 10 μM reverse primer, 1 μL of 0.005 ng/μL or 50 ng/μL RNA sample, and RNase free water up to 10 μL. qRT-PCR reactions were performed with ViiA7 thermocyclers (Applied Biosystems) according to Luna universal One-Step RT-qPCR kit recommendations. Default melt curve settings for the thermocycler were used.

Control reactions lacking RNA were performed for each primer pair and reactions lacking the RT mix were performed for each RNA sample. After ensuring detection of *glgC*, *pgaA*, *phoB*, and *secA* mRNA targets in 50 ng RNA and CsrB, McaS, SgrS and 16s RNA targets in 0.005 ng RNA with single-peak melt curves, the $\Delta\Delta C_T$ method was used to determine relative change in RNA level upon sRNA induction. ΔC_T values were calculated for mRNAs relative to the *secA* mRNA reference and for sRNAs relative to the 16s rRNA reference for each biological replicate. Paired two-tailed t-tests between uninduced and induced ΔC_T values of a given RNA target were used to determine significant changes in RNA abundance (upon induction of a sRNA). $\Delta\Delta C_T$ values were calculated, averaged across biological replicas, and presented as log2 fold changes.

Congo red plate assay

Wild type and cured $\Delta mcaS$ K-12 MG1655 *E. coli* strains were made competent according to lab protocols. Wild type and mutant McaS (5′-most GGA:CCA mutant; Supplementary Tables S1–S4), cloned in the low copy number pBTRK-pLacO-Empty plasmid (Youngquist et al., 2013; Hernandez-Lozada et al., 2018), were transformed into the $\Delta mcaS$ strain. An empty control pBTRK-pLacO-Empty plasmid was transformed into both the wild type and $\Delta mcaS$ strains. Single colonies were grown up in biological triplicate 5 mL LB cultures. 10 μL of each saturated overnight culture was spread on Congo red agar plates and grown at room temperature for 36–48 h. Plates were placed on a UV to white light conversion screen (BioRad) and backlit with LED lighting for imaging.

Fluorescence assays with induction of genomic Spot42

To evaluate the biological relevance of CsrA impacting the Spot 42-*fucP* interaction, culturing conditions were developed to

allow native expression of the Spot 42 sRNA in K-12 MG1655 *E. coli* to regulate *fucP-gfp* reporters expressed from the low copy number pBTRK-pLacO (CmR) plasmid. The media utilized was M9 Media supplemented with 0.4% glycerol, 0.2% casamino acids, 10 μg/mL thiamine, 2 mM MgSO4, and 0.1 mM CaCl2, which has been previously demonstrated to allow for high genomic expression of the Spot 42 sRNA upon bolus addition of 0.2% glucose (Beisel and Storz, 2011). For the fluorescence assay, the pBTRK-pLaco-*fucP-gfp* (CmR) plasmids containing wild type and mutant *fucP* 5' UTRs with disrupted Spot 42 binding sites (Supplementary Tables S1–S4) were transformed into wild type and *Δspf* K-12 MG1655 *E. coli* strains. Single colonies were grown overnight in 5 mL of the M9 Media in biological triplicate until saturation and seeded for culturing by diluting 1:100 into 25 mL of the M9 Media. Additionally, the *fucP*-GFP reporter was induced at seeding using IPTG at a final concentration of 1 mM. Bolus glucose was added to a final concentration of 0.2% at an OD600 of 0.2, approximately 3.5 h after seeding. The cultures were then sampled at various timepoints following induction and fluorescence was measured using a BioTek Cytation3 with an excitation wavelength of 488 nm and an emission wavelength of 513 nm. Absorbance at 600 nm was also measured and the fluorescent values were normalized to control for differences in number of cells per well. Average fluorescence values of each *fucP-gfp* reporter were compared between wild type and *Δspf* strains with heteroscedastic two-tailed t-tests (n = 3, P-val <0.05) to determine significant regulation by genomic Spot42. To compare Spot42 regulation of different *fucP-gfp* reporter constructs, fold change in fluorescence for each construct was determined as the ratio between average median fluorescence in the wild type and *Δspf* strains (n = 3). Heteroscedastic two-tailed t-tests were utilized to determine if fluorescence fold changes were significantly different (P-val <0.05) between the *fucP-gfp* constructs.

Data availability statement

The original contributions presented in the study are included in the article/Supplementary Material, further inquiries can be directed to the corresponding author.

Author contributions

AMR-N, TS, AL, and MM designed the study, ran the experiments, collected and analyzed data, and prepared the manuscript. RB, AE, IJ, and NC ran experiments. LC designed the study, and prepared the manuscript. All authors contributed to the article and approved the submitted version.

Funding

Acknowledgments

Conflict of interest

The authors declare that the research was conducted in the absence of any commercial or financial relationships that could be construed as a potential conflict of interest.

Publisher's note

All claims expressed in this article are solely those of the authors and do not necessarily represent those of their affiliated organizations, or those of the publisher, the editors and the reviewers. Any product that may be evaluated in this article, or claim that may be made by its manufacturer, is not guaranteed or endorsed by the publisher.

Supplementary material

The Supplementary Material for this article can be found online at: https://www.frontiersin.org/articles/10.3389/fmolb.2023.1249528/full#supplementary-material

References

Adamson, D. N., and Lim, H. N. (2013). Rapid and robust signaling in the CsrA cascade via RNA–protein interactions and feedback regulation. *Proc. Natl. Acad. Sci. U. S. A.* 110 (32), 13120–13125. doi:10.1073/pnas.1308476110

Andreassen, P. R., Pettersen, J. S., Szczerba, M., Valentin-Hansen, P., Møller-Jensen, J., and Jørgensen, M. G. (2018). sRNA-dependent control of curli biosynthesis in *Escherichia coli*: mcaS directs endonucleolytic cleavage of csgD mRNA. *Nucleic Acids Res.* 46 (13), 6746–6760. doi:10.1093/nar/gky479

Aoyama, J. J., Raina, M., Zhong, A., and Storz, G. (2022). Dual-function Spot 42 RNA encodes a 15–amino acid protein that regulates the CRP transcription factor. *Proc. Natl. Acad. Sci.* 119(10), e2119866119. doi:10.1073/pnas.2119866119

Azam, M. S., and Vanderpool, C. K. (2017). Translational regulation by bacterial small RNAs via an unusual Hfq-dependent mechanism. *Nucleic Acids Res.* 46 (5), 2585–2599. doi:10.1093/nar/gkx1286

Bak, G., Lee, J., Suk, S., Kim, D., Young Lee, J., Kim, K., et al. (2015). Identification of novel sRNAs involved in biofilm formation, motility and fimbriae formation in *Escherichia coli*. *Sci. Rep.* 5 (1), 15287. doi:10.1038/srep15287

Baker, C. S., Eory, L. A., Yakhnin, H., Mercante, J., Romeo, T., and Babitzke, P. (2007). CsrA inhibits translation initiation of *Escherichia coli* hfq by binding to a single site overlapping the Shine-Dalgarno sequence. *J. Bacteriol.* 189 (15), 5472–5481. doi:10.1128/jb.00529-07

Baker, C. S., Morozov, I., Suzuki, K., Romeo, T., and Babitzke, P. (2002). CsrA regulates glycogen biosynthesis by preventing translation of glgC in *Escherichia coli*. *Mol. Microbiol.* 44 (6), 1599–1610. doi:10.1046/j.1365-2958.2002.02982.x

Beisel, C. L., and Storz, G. (2011). The base-pairing RNA spot 42 participates in a multioutput feedforward loop to help enact catabolite repression in *Escherichia coli*. *Mol. Cell* 41 (3), 286–297. doi:10.1016/j.molcel.2010.12.027

Beisel, C. L., Updegrove, T. B., Janson, B. J., and Storz, G. (2012). Multiple factors dictate target selection by Hfq-binding small RNAs. *EMBO J.* 31 (8), 1961–1974. doi:10.1038/emboj.2012.52

Bobrovskyy, M., Azam, M. S., Frandsen, J. K., Zhang, J., Poddar, A., Ma, X., et al. (2019). Determinants of target prioritization and regulatory hierarchy for the bacterial small RNA SgrS. *Mol. Microbiol.* 112 (4), 1199–1218. doi:10.1111/mmi.14355

Boysen, A., Møller-Jensen, J., Kallipolitis, B., Valentin-Hansen, P., and Overgaard, M. (2010). Translational regulation of gene expression by an anaerobically induced small non-coding RNA in *Escherichia coli*. *J. Biol. Chem.* 285 (14), 10690–10702. doi:10.1074/jbc.M109.089755

Brantl, S., and Jahn, N. (2015). sRNAs in bacterial type I and type III toxin-antitoxin systems. *FEMS Microbiol. Rev.* 39 (3), 413–427. doi:10.1093/femsre/fuv003

Busch, A., Richter, A. S., and Backofen, R. (2008). IntaRNA: efficient prediction of bacterial sRNA targets incorporating target site accessibility and seed regions. *Bioinformatics* 24 (24), 2849–2856. doi:10.1093/bioinformatics/btn544

Butz, H. A., Mey, A. R., Ciosek, A. L., and Payne, S. M. (2019). *Vibrio cholerae* CsrA directly regulates varA to increase expression of the three nonredundant Csr small RNAs. *MBio* 10 (3). doi:10.1128/mBio.01042-19

Caillet, J., Baron, B., Boni, I. V., Caillet-Saguy, C., and Hajnsdorf, E. (2019). Identification of protein-protein and ribonucleoprotein complexes containing Hfq. *Sci. Rep.* 9 (1), 14054. doi:10.1038/s41598-019-50562-w

Cameron, T. A., Matz, L. M., Sinha, D., and De Lay, N. R. (2019). Polynucleotide phosphorylase promotes the stability and function of Hfq-binding sRNAs by degrading target mRNA-derived fragments. *Nucleic Acids Res.* 47 (16), 8821–8837. doi:10.1093/nar/gkz616

Cherepanov, P. P., and Wackernagel, W. (1995). Gene disruption in *Escherichia coli*: tcR and KmR cassettes with the option of Flp-catalyzed excision of the antibiotic-resistance determinant. *Gene* 158 (1), 9–14. doi:10.1016/0378-1119(95)00193-A

Cho, S. H., Lei, R., Henninger, T. D., and Contreras, L. M. (2014). Discovery of ethanol responsive small RNAs in Zymomonas mobilis. *Appl. Environ. Microbiol.* 80 (14), 4189–4198. doi:10.1128/aem.00429-14

Datsenko, K. A., and Wanner, B. L. (2000). One-step inactivation of chromosomal genes in *Escherichia coli* K-12 using PCR products. *Proc. Natl. Acad. Sci.* 97 (12), 6640–6645. doi:10.1073/pnas.120163297

Darnell, R. B. (2010). HITS-CLIP: panoramic views of protein-RNA regulation in living cells. *Wiley Interdiscip. Rev. RNA* 1 (2), 266–286. doi:10.1002/wrna.31

De Lay, N., Schu, D. J., and Gottesman, S. (2013). Bacterial small RNA-based negative regulation: hfq and its accomplices. *J. Biol. Chem.* 288 (12), 7996–8003. doi:10.1074/jbc.R112.441386

Desnoyers, G., and Massé, E. (2012). Noncanonical repression of translation initiation through small RNA recruitment of the RNA chaperone Hfq. *Genes and Dev.* 26 (7), 726–739. doi:10.1101/gad.182493.111

DiChiara, J. M., Contreras-Martinez, L. M., Livny, J., Smith, D., McDonough, K. A., and Belfort, M. (2010). Multiple small RNAs identified in Mycobacterium bovis BCG are also expressed in *Mycobacterium tuberculosis* and Mycobacterium smegmatis. *Nucleic acids Res.* 38 (12), 4067–4078. doi:10.1093/nar/gkq101

Dubey, A. K., Baker, C. S., Romeo, T., and Babitzke, P. (2005). RNA sequence and secondary structure participate in high-affinity CsrA-RNA interaction. *RNA* 11 (10), 1579–1587. doi:10.1261/rna.2990205

Dubey, A. K., Baker, C. S., Suzuki, K., Jones, A. D., Pandit, P., Romeo, T., et al. (2003). CsrA regulates translation of the *Escherichia coli* carbon starvation gene, cstA, by blocking ribosome access to the cstA transcript. *J. Bacteriol.* 185 (15), 4450–4460. doi:10.1128/JB.185.15.4450-4460.2003

Durand, S., and Storz, G. (2010). Reprogramming of anaerobic metabolism by the FnrS small RNA. *Mol. Microbiol.* 75(5), 1215–1231. doi:10.1111/j.1365-2958.2010.07044.x

Espah Borujeni, A., Cetnar, D., Farasat, I., Smith, A., Lundgren, N., and Salis, H. M. (2017). Precise quantification of translation inhibition by mRNA structures that overlap with the ribosomal footprint in N-terminal coding sequences. *Nucleic Acids Res.* 45 (9), 5437–5448. doi:10.1093/nar/gkx061

Finn, R. D., Bateman, A., Clements, J., Coggill, P., Eberhardt, R. Y., Eddy, S. R., et al. (2014). Pfam: the protein families database. *Nucleic acids Res.* 42, D222–D230. doi:10.1093/nar/gkt1223

Fozo, E. M., Kawano, M., Fontaine, F., Kaya, Y., Mendieta, K. S., Jones, K. L., et al. (2008). Repression of small toxic protein synthesis by the Sib and OhsC small RNAs. *Mol. Microbiol.* 70 (5), 1076–1093. doi:10.1111/j.1365-2958.2008.06394.x

Gebhardt, M. J., Kambara, T. K., Ramsey, K. M., and Dove, S. L. (2020). Widespread targeting of nascent transcripts by RsmA in *Pseudomonas aeruginosa*. *Proc. Natl. Acad. Sci.* 117, 10520. doi:10.1073/pnas.1917587117

Gelderman, G., Sivakumar, A., Lipp, S., and Contreras, L. M. (2015). Adaptation of Tri-molecular fluorescence complementation allows assaying of regulatory Csr RNA-protein interactions in bacteria. *Biotechnol. Bioeng.* 112 (2), 365–375. doi:10.1002/bit.25351

Gerrick, E. R., Barbier, T., Chase, M. R., Xu, R., François, J., Lin, V. H., et al. (2018). Small RNA profiling in *Mycobacterium tuberculosis* identifies MrsI as necessary for an anticipatory iron sparing response. *Proc. Natl. Acad. Sci.* 115 (25), 6464–6469. doi:10.1073/pnas.1718003115

Gottesman, S., McCullen, C., Guillier, M., Vanderpool, C., Majdalani, N., Benhammou, J., et al. (2006). Small RNA regulators and the bacterial response to stress. *Cold Spring Harb. Symposia Quantitative Biol.* 71, 1–11. doi:10.1101/sqb.2006.71.016

Gottesman, S., and Storz, G. (2011). Bacterial small RNA regulators: versatile roles and rapidly evolving variations. *Cold Spring Harb. Perspect. Biol.* 3 (12). doi:10.1101/cshperspect.a003798

Gruber, A. R., Lorenz, R., Bernhart, S. H., Neuböck, R., and Hofacker, I. L. (2008). The Vienna RNA websuite. *Nucleic Acids Res.* 36 (2), W70–W74. doi:10.1093/nar/gkn188

Guo, M. S., Updegrove, T. B., Gogol, E. B., Shabalina, S. A., Gross, C. A., and Storz, G. (2014). MicL, a new sigmaE-dependent sRNA, combats envelope stress by repressing synthesis of Lpp, the major outer membrane lipoprotein. *Genes and Dev.* 28 (14), 1620–1634. doi:10.1101/gad.243485.114

Haning, K., Cho, S. H., and Contreras, L. M. (2014). Small RNAs in mycobacteria: an unfolding story. *Front. Cell. Infect. Microbiol.* 4, 96. doi:10.3389/fcimb.2014.00096

Hernández Lozada, N. J., Lai, R.-Y., Simmons, T. R., Thomas, K. A., Chowdhury, R., Maranas, C. D., et al. (2018). Highly active C8-acyl-ACP thioesterase variant isolated by a synthetic selection strategy. *ACS Synth. Biol.* 7 (9), 2205–2215. doi:10.1021/acssynbio.8b00215

Holmqvist, E., Li, L., Bischler, T., Barquist, L., and Vogel, J. (2018). Global maps of ProQ binding *in vivo* reveal target recognition via RNA structure and stability control at mRNA 3′ ends. *Mol. Cell* 70 (5), 971–982.e6. doi:10.1016/j.molcel.2018.04.017

Holmqvist, E., and Vogel, J. (2018). RNA-binding proteins in bacteria. *Nat. Rev. Microbiol.* 16 (10), 601–615. doi:10.1038/s41579-018-0049-5

Holmqvist, E., Wright, P. R., Li, L., Bischler, T., Barquist, L., Reinhardt, R., et al. (2016). Global RNA recognition patterns of post-transcriptional regulators Hfq and CsrA revealed by UV crosslinking *in vivo*. *EMBO J.*, 991–1011. doi:10.15252/embj.201593360

Hör, J., Matera, G., Vogel, J., Gottesman, S., and Storz, G. (2020). Trans-acting small RNAs and their effects on gene expression in *Escherichia coli* and *Salmonella enterica*. *EcoSal Plus* 9. doi:10.1128/ecosalplus.ESP-0030-2019

Hör, J., Garriss, G., Di Giorgio, S., Hack, L.-M., Vanselow, J. T., Förstner, K. U., et al. (2020). Grad-seq in a Gram-positive bacterium reveals exonucleolytic sRNA activation in competence control. *EMBO J.* 2020, e103852. doi:10.15252/embj.2019103852

Hör, J., Gorski, S. A., and Vogel, J. (2018). Bacterial RNA biology on a genome scale. *Mol. Cell*. doi:10.1016/j.molcel.2017.12.023

Iosub, I. A., van Nues, R. W., McKellar, S. W., Nieken, K. J., Marchioretto, M., Sy, B., et al. (2020). Hfq CLASH uncovers sRNA-target interaction networks linked to nutrient availability adaptation. *ELife* 9, e54655. doi:10.7554/eLife.54655

Jorgensen, M. G., Thomason, M. K., Havelund, J., Valentin-Hansen, P., and Storz, G. (2013). Dual function of the McaS small RNA in controlling biofilm formation. *Genes Dev.* 27 (10), 1132–1145. doi:10.1101/gad.214734.113

Kajitani, M., Kato, A., Wada, A., Inokuchi, Y., and Ishihama, A. (1994). Regulation of the *Escherichia coli* hfq gene encoding the host factor for phage Q beta. *J. Bacteriol.* 176 (2), 531–534. doi:10.1128/jb.176.2.531-534.1994

Kavita, K., de Mets, F., and Gottesman, S. (2018). New aspects of RNA-based regulation by Hfq and its partner sRNAs. *Curr. Opin. Microbiol.* 42, 53–61. doi:10.1016/j.mib.2017.10.014

Kulkarni, P. R., Jia, T., Kuehne, S. A., Kerkering, T. M., Morris, E. R., Searle, M. S., et al. (2014). A sequence-based approach for prediction of CsrA/RsmA targets in bacteria with experimental validation in *Pseudomonas aeruginosa*. *Nucleic Acids Res.* 42 (11), 6811–6825. doi:10.1093/nar/gku309

Lai, Y.-J., Yakhnin, H., Pannuri, A., Pourciau, C., Babitzke, P., and Romeo, T. (2022). CsrA regulation via binding to the base-pairing small RNA Spot 42. *Mol. Microbiol.* 117, 32–53. doi:10.1111/mmi.14769

Lalaouna, D., Carrier, M.-C., Semsey, S., Brouard, J.-S., Wang, J., Wade, J. T., et al. (2015). A 3′ external transcribed spacer in a tRNA transcript acts as a sponge for small RNAs to prevent transcriptional noise. *Mol. Cell* 58 (3), 393–405. doi:10.1016/j.molcel. 2015.03.013

Lamm-Schmidt, V., Fuchs, M., Sulzer, J., Gerovac, M., Hör, J., Dersch, P., et al. (2021). Grad-seq identifies KhpB as a global RNA-binding protein in *Clostridioides difficile* that regulates toxin production. *microLife* 2, uqab004. doi:10.1093/femsml/uqab004

Leistra, A. N., Amador, P., Buvanendiran, A., Moon-Walker, A., and Contreras, L. M. (2017). Rational modular RNA engineering based on *in vivo* profiling of structural accessibility. *ACS Synth. Biol.* 6, 2228. doi:10.1021/acssynbio.7b00185

Leistra, A. N., Curtis, N. C., and Contreras, L. M. (2019). Regulatory non-coding sRNAs in bacterial metabolic pathway engineering. *Metab. Eng.* 52, 190–214. doi:10.1016/j.ymben.2018.11.013

Leistra, A. N., Gelderman, G., Sowa, S. W., Moon-Walker, A., Salis, H. M., and Contreras, L. M. (2018). A canonical biophysical model of the CsrA global regulator suggests flexible regulator-target interactions. *Sci. Rep.* 8 (1), 9892. doi:10.1038/s41598-018-27474-2

Leistra, A. N., Mihailovic, M. K., and Contreras, L. M. (2018). Fluorescence-based methods for characterizing RNA interactions *in vivo*. *Methods Mol. Biol.* 1737. doi:10.1007/978-1-4939-7634-8_9

Leng, Y., Vakulskas, C. A., Zere, T. R., Pickering, B. S., Watnick, P. I., Babitzke, P., et al. (2016). Regulation of CsrB/C sRNA decay by EIIA(Glc) of the phosphoenolpyruvate: carbohydrate phosphotransferase system. *Mol. Microbiol.* 99 (4), 627–639. doi:10.1111/mmi.13259

Liu, M. Y., Gui, G., Wei, B., Preston, J. F., 3rd, Oakford, L., Yuksel, U., et al. (1997). The RNA molecule CsrB binds to the global regulatory protein CsrA and antagonizes its activity in *Escherichia coli*. *J. Biol. Chem.* 272 (28), 17502–17510. doi:10.1074/jbc.272.28. 17502

Liu, M. Y., and Romeo, T. (1997). The global regulator CsrA of *Escherichia coli* is a specific mRNA-binding protein. *J. Bacteriol.* 179 (14), 4639–4642. doi:10.1128/jb.179. 14.4639-4642.1997

Liu, T., Zhang, K., Xu, S., Wang, Z., Fu, H., Tian, B., et al. (2017). Detecting RNA-RNA interactions in *E. coli* using a modified CLASH method. *BMC Genomics* 18 (1), 343. doi:10.1186/s12864-017-3725-3

Lorenz, R., Bernhart, S. H., Honer Zu Siederdissen, C., Tafer, H., Flamm, C., Stadler, P. F., et al. (2011). ViennaRNA package 2.0. *Algorithms Mol. Biol.* 6, 26. doi:10.1186/1748-7188-6-26

Lukasiewicz, A. J., and Contreras, L. M. (2020). Antisense probing of dynamic RNA structures. *Methods (San Diego, Calif.)* 183, 76–83. doi:10.1016/j.ymeth.2020.01.015

Maki, K., Uno, K., Morita, T., and Aiba, H. (2008). RNA, but not protein partners, is directly responsible for translational silencing by a bacterial Hfq-binding small RNA. *Proc. Natl. Acad. Sci.* 105 (30), 10332–10337. doi:10.1073/pnas.0803106105

Mann, M., Wright, P. R., and Backofen, R. (2017). IntaRNA 2.0: enhanced and customizable prediction of RNA–RNA interactions. *Nucleic Acids Res.* 45 (W1), W435–W439. doi:10.1093/nar/gkx279

Mehrer, C. R., Incha, M. R., Politz, M. C., and Pfleger, B. F. (2018). Anaerobic production of medium-chain fatty alcohols via a β-reduction pathway. *Metab. Eng.* 48, 63–71. doi:10.1016/j.ymben.2018.05.011

Melamed, S., Adams, P. P., Zhang, A., Zhang, H., and Storz, G. (2020). RNA-RNA interactomes of ProQ and hfq reveal overlapping and competing roles. *Mol. Cell* 77 (2), 411–425.e7. doi:10.1016/j.molcel.2019.10.022

Melamed, S., Peer, A., Faigenbaum-Romm, R., Gatt, Y. E., Reiss, N., Bar, A., et al. (2016). Global mapping of small RNA-target interactions in bacteria. *Mol. Cell* 63 (5), 884–897. doi:10.1016/j.molcel.2016.07.026

Mercante, J., Edwards, A. N., Dubey, A. K., Babitzke, P., and Romeo, T. (2009). Molecular geometry of CsrA (RsmA) binding to RNA and its implications for regulated expression. *J. Mol. Biol.* 392 (2), 511–528. doi:10.1016/j.jmb.2009.07.034

Mihailovic, M. K., Ekdahl, A. M., Chen, A., Leistra, A. N., Li, B., González Martínez, J., et al. (2021). Uncovering transcriptional regulators and targets of sRNAs using an integrative data-mining approach: H-NS-regulated RseX as a Case Study. *Front. Cell. Infect. Microbiol.* 11, 656533. doi:10.3389/fcimb.2021.696533

Mihailovic, M. K., Vazquez-Anderson, J., Li, Y., Fry, V., Vimalathas, P., Herrera, D., et al. (2018). High-throughput *in vivo* mapping of RNA accessible interfaces to identify functional sRNA binding sites. *Nat. Commun.* 9 (1), 4084. doi:10.1038/s41467-018-06207-z

Miyakoshi, M., Matera, G., Maki, K., Sone, Y., and Vogel, J. (2019). Functional expansion of a TCA cycle operon mRNA by a 3 end-derived small RNA. *Nucleic Acids Res.* 47 (4), 2075–2088. doi:10.1093/nar/gky1243

Moon, K., and Gottesman, S. (2011). Competition among Hfq-binding small RNAs in *Escherichia coli*. *Mol. Microbiol.* 82(6), 1545–1562. doi:10.1111/j.1365-2958.2011. 07907.x

Morita, T., Mochizuki, Y., and Aiba, H. (2006). Translational repression is sufficient for gene silencing by bacterial small noncoding RNAs in the absence of mRNA destruction. *Proc. Natl. Acad. Sci.* 103 (13), 4858–4863. doi:10.1073/pnas.0509638103

Müller, P., Gimpel, M., Wildenhain, T., and Brantl, S. (2019). A new role for CsrA: promotion of complex formation between an sRNA and its mRNA target in Bacillus subtilis. *RNA Biol.* 16 (7), 972–987. doi:10.1080/15476286.2019.1605811

Na, D., Yoo, S. M., Chung, H., Park, H., Park, J. H., and Lee, S. Y. (2013). Metabolic engineering of *Escherichia coli* using synthetic small regulatory RNAs. *Nat. Biotechnol.* 31 (2), 170–174. doi:10.1038/nbt.2461

Nitzan, M., Rehani, R., and Margalit, H. (2017). Integration of bacterial small RNAs in regulatory networks. *Annu. Rev. Biophysics* 46 (1), 131–148. doi:10.1146/annurev-biophys-070816-034058

Noh, M., Yoo, S. M., Kim, W. J., and Lee, S. Y. (2017). Gene expression knockdown by modulating synthetic small RNA expression in *Escherichia coli*. *Cell Syst.* 5 (4), 418–426. doi:10.1016/j.cels.2017.08.016

Olejniczak, M., Jiang, X., Basczok, M. M., and Storz, G. (2022). KH domain proteins: another family of bacterial RNA matchmakers? *Mol. Microbiol.* 117 (1), 10–19. doi:10.1111/mmi.14842

Pannuri, A., Yakhnin, H., Vakulskas, C. A., Edwards, A. N., Babitzke, P., and Romeo, T. (2012). Translational repression of NhaR, a novel pathway for multi-tier regulation of biofilm circuitry by CsrA. *J. Bacteriol.* 194 (1), 79–89. doi:10.1128/jb.06209-11

Park, H., McGibbon, L. C., Potts, A. H., Yakhnin, H., Romeo, T., and Babitzke, P. (2017). Translational repression of the RpoS antiadapter IraD by CsrA is mediated via translational coupling to a short upstream open reading frame. *MBio* 8 (4). doi:10.1128/mBio.01355-17

Parker, A., Cureoglu, S., De Lay, N., Majdalani, N., and Gottesman, S. (2017). Alternative pathways for *Escherichia coli* biofilm formation revealed by sRNA overproduction. *Mol. Microbiol.* 2017. doi:10.1111/mmi.13702

Patterson-Fortin, L. M., Vakulskas, C. A., Yakhnin, H., Babitzke, P., and Romeo, T. (2013). Dual posttranscriptional regulation via a cofactor-responsive mRNA leader. *J. Mol. Biol.* 425 (19), 3662–3677. doi:10.1016/j.jmb.2012.12.010

Peng, P. Y. (2014). *Structural models of bacterial RNA chaperone hfq in complex with the RNA targets*. United States: Johns Hopkins University.

Potts, A. H., Vakulskas, C. A., Pannuri, A., Yakhnin, H., Babitzke, P., and Romeo, T. (2017). Global role of the bacterial post-transcriptional regulator CsrA revealed by integrated transcriptomics. *Nat. Commun.* 8 (1), 1596. doi:10.1038/s41467-017-01613-1

Prevost, K., Desnoyers, G., Jacques, J.-F., Lavoie, F., and Masse, E. (2011). Small RNA-induced mRNA degradation achieved through both translation block and activated cleavage. *Genes and Dev.* 25 (4), 385–396. doi:10.1101/gad.2001711

Ren, B., Shen, H., Lu, Z. J., Liu, H., and Xu, Y. (2014). The phzA2-G2 transcript exhibits direct RsmA-mediated activation in *Pseudomonas aeruginosa* M18. *PloS one* 9 (2), e89653. doi:10.1371/journal.pone.0089653

Renda, A., Poly, S., Lai, Y. J., Pannuri, A., Yakhnin, H., Potts, A. H., et al. (2020). CsrA-mediated translational activation of *ymdA* expression in *Escherichia coli*. *mBio* 11 (5), 008499–e920. doi:10.1128/mBio.00849-20

Romeo, T., and Babitzke, P. (2018). Global regulation by CsrA and its RNA antagonists. *Microbiol. Spectr.* 6(2), doi:10.1128/microbiolspec.RWR-0009–2017

Romeo, T., Vakulskas, C. A., and Babitzke, P. (2013). Post-transcriptional regulation on a global scale: form and function of Csr/Rsm systems. *Environ. Microbiol.* 15 (2), 313–324. doi:10.1111/j.1462-2920.2012.02794.x

Sahagan, B. G., and Dahlberg, J. E. (1979). A small, unstable RNA molecule of *Escherichia coli*: spot 42 RNA: II. Accumulation and distribution. *J. Mol. Biol.* 131 (3), 593–605. doi:10.1016/0022-2836(79)90009-3

Salvail, H., Lanthier-Bourbonnais, P., Sobota, J. M., Caza, M., Benjamin, J. A., Mendieta, M. E., et al. (2010). A small RNA promotes siderophore production through transcriptional and metabolic remodeling. *Proc. Natl. Acad. Sci. U. S. A.* 107 (34), 15223–15228. doi:10.1073/pnas.1007805107

Santiago-Frangos, A., Kavita, K., Schu, D. J., Gottesman, S., and Woodson, S. A. (2016). C-terminal domain of the RNA chaperone Hfq drives sRNA competition and release of target RNA. *Proc. Natl. Acad. Sci. U. S. A.* 113 (41), E6089–E6096. doi:10.1073/pnas.1613053113

Santiago-Frangos, A., and Woodson, S. A. (2018). Hfq chaperone brings speed dating to bacterial sRNA. *Wiley Interdiscip. Rev. RNA* 9 (4), e1475. doi:10.1002/wrna.1475

Smirnov, A., Förstner, K. U., Holmqvist, E., Otto, A., Günster, R., Becher, D., et al. (2016). Grad-seq guides the discovery of ProQ as a major small RNA-binding protein. *Proc. Natl. Acad. Sci.* 113 (41), 11591–11596. doi:10.1073/pnas.1609981113

Smirnov, A., Wang, C., Drewry, L. L., and Vogel, J. (2017). Molecular mechanism of mRNA repression in trans by a ProQ-dependent small RNA. *EMBO J.* 36 (8), 1029–1045. doi:10.15252/embj.201696127

Sowa, S. W., Gelderman, G., Leistra, A. N., Buvanendiran, A., Lipp, S., Pitaktong, A., et al. (2017). Integrative FourD omics approach profiles the target network of the carbon storage regulatory system. *Nucleic Acids Res.* 45 (4), 1673–1686. doi:10.1093/nar/gkx048

Taneja, S., and Dutta, T. (2019). On a stake-out: mycobacterial small RNA identification and regulation. *Non-Coding RNA Res.* 4 (3), 86–95. doi:10.1016/j.ncrna.2019.05.001

Thomason, M. K., Fontaine, F., De Lay, N., and Storz, G. (2012). A small RNA that regulates motility and biofilm formation in response to changes in nutrient availability in *Escherichia coli*. *Mol. Microbiol.* 84 (1), 17–35. doi:10.1111/j.1365-2958.2012.07965.x

Tsai, C.-H., Liao, R., Chou, B., and Contreras, L. M. (2015). Transcriptional analysis of Deinococcus radiodurans reveals novel small RNAs that are differentially expressed under ionizing radiation. *Appl. Environ. Microbiol.* 81 (5), 1754–1764. doi:10.1128/AEM.03709-14

Vakulskas, C. A., Potts, A. H., Babitzke, P., Ahmer, B. M. M., and Romeo, T. (2015). Regulation of bacterial virulence by Csr (Rsm) systems. *Microbiol. Mol. Biol. Rev.* 79 (2), 193–224. doi:10.1128/mmbr.00052-14

Vanderpool, C. K., and Gottesman, S. (2004). Involvement of a novel transcriptional activator and small RNA in post-transcriptional regulation of the glucose phosphoenolpyruvate phosphotransferase system. *Mol. Microbiol.* 54 (4), 1076–1089. doi:10.1111/j.1365-2958.2004.04348.x

Vazquez-Anderson, J., and Contreras, L. M. (2013). Regulatory RNAs: charming gene management styles for synthetic biology applications. *RNA Biol.* 10 (12), 1778–1797. doi:10.4161/rna.27102

Villa, J. K., Han, R., Tsai, C. H., Chen, A., Sweet, P., Franco, G., et al. (2021). A small RNA regulates pprM, a modulator of pleiotropic proteins promoting DNA repair, in Deinococcus radiodurans under ionizing radiation. *Sci. Rep.* 11 (1), 12949. doi:10.1038/s41598-021-91335-8

Villa, J. K., Su, Y., Contreras, L. M., and Hammond, M. C. (2017). Synthetic biology of small RNAs and riboswitches. *Microbiol. Spectr.* 6 (3). doi:10.1128/microbiolspec.RWR-0007-2017

Vogel, J., and Luisi, B. F. (2011). Hfq and its constellation of RNA. *Nat. Rev. Micro* 9 (8), 578–589. doi:10.1038/nrmicro2615

Wadler, C. S., and Vanderpool, C. K. (2007). A dual function for a bacterial small RNA: sgrS performs base pairing-dependent regulation and encodes a functional polypeptide. *Proc. Natl. Acad. Sci. U. S. A.* 104 (51), 20454–20459. doi:10.1073/pnas.0708102104

Wagner, E. G. H. (2013). Cycling of RNAs on hfq. *RNA Biol.* 10 (4), 619–626. doi:10.4161/rna.24044

Wagner, E. G. H., and Romby, P. (2015). "Chapter three - small RNAs in bacteria and archaea: who they are, what they do, and how they do it," in *Advances in genetics*. Editors T. Friedmann, J. C. Dunlap, and S. F. Goodwin (Cambridge, Massachusetts, United States: Academic Press), 90, 133–208. doi:10.1016/bs.adgen.2015.05.001

Wang, J., Liu, T., Zhao, B., Lu, Q., Wang, Z., Cao, Y., et al. (2016). sRNATarBase 3.0: an updated database for sRNA-target interactions in bacteria. *Nucleic Acids Res.* 44 (D1), D248–D253. doi:10.1093/nar/gkv1127

Wang, X., Dubey, A. K., Suzuki, K., Baker, C. S., Babitzke, P., and Romeo, T. (2005). CsrA post-transcriptionally represses pgaABCD, responsible for synthesis of a biofilm polysaccharide adhesin of *Escherichia coli*. *Mol. Microbiol.* 56 (6), 1648–1663. doi:10.1111/j.1365-2958.2005.04648.x

Waters, S. A., McAteer, S. P., Kudla, G., Pang, I., Deshpande, N. P., Amos, T. G., et al. (2017). Small RNA interactome of pathogenic *E. coli* revealed through crosslinking of RNase E. *EMBO J.* 36 (3), 374–387. doi:10.15252/embj.201694639

Weilbacher, T., Suzuki, K., Dubey, A. K., Wang, X., Gudapaty, S., Morozov, I., et al. (2003). A novel sRNA component of the carbon storage regulatory system of *Escherichia coli*. *Mol. Microbiol.* 48 (3), 657–670. doi:10.1046/j.1365-2958.2003.03459.x

Yakhnin, A. V., Yakhnin, H., and Babitzke, P. (2012). Gel mobility shift assays to detect protein-RNA interactions. *Methods Mol. Biol. Clift. N.J.)* 905, 201–211. doi:10.1007/978-1-61779-949-5_12

Yakhnin, H., Aichele, R., Ades, S. E., Romeo, T., and Babitzke, P. (2017). Circuitry linking the global Csr and σE-dependent cell envelope stress response systems. *J. Bacteriol.* doi:10.1128/jb.00484-17

Yakhnin, H., Baker, C. S., Berezin, I., Evangelista, M. A., Rassin, A., Romeo, T., et al. (2011). CsrA represses translation of sdiA, which encodes the N-Acylhomoserine-l-Lactone receptor of *Escherichia coli*, by binding exclusively within the coding region of sdiA mRNA. *J. Bacteriol.* 193 (22), 6162–6170. doi:10.1128/JB.05975-11

Yakhnin, H., Yakhnin, A. V., Baker, C. S., Sineva, E., Berezin, I., Romeo, T., et al. (2011). Complex regulation of the global regulatory gene csrA: csrA-mediated translational repression, transcription from five promoters by Eσ(70) and Eσ(S), and indirect transcriptional activation by CsrA. *Mol. Microbiol.* 81 (3), 689–704. doi:10.1111/j.1365-2958.2011.07723.x

Youngquist, J. T., Schumacher, M. H., Rose, J. P., Raines, T. C., Politz, M. C., Copeland, M. F., et al. (2013). Production of medium chain length fatty alcohols from glucose in *Escherichia coli*. *Metab. Eng.* 20, 177–186. doi:10.1016/j.ymben.2013.10.006